Accessibility and recovery assessment of Houston's roadway network due to fluvial flooding during Hurricane Harvey

Avantika Gori[§1], Ioannis Gidaris, A.M. ASCE[§2], James R. Elliott[3], Jamie Padgett A.M. ASCE[4], Kevin Loughran[5], Philip Bedient[6], Pranavesh Panakkal[7] and Andrew Juan[8]

Abstract: The record-breaking rainfall produced by Hurricane Harvey resulted in catastrophic and prolonged impacts on Houston's transportation infrastructure, inundating entire neighborhoods and rendering them inaccessible to emergency response services. Harvey highlighted the vulnerability of the roadway network to severe inundation during extreme fluvial flood events and emphasized the need for detailed roadway network accessibility characterization in order to determine which areas of the city are most vulnerable and sensitive to transportation disruption. This study poses an integrated framework to evaluate fluvial flood impacts on roadway accessibility to emergency services experienced by potentially socially vulnerable populations. This framework is applied to assess the time evolution of road network accessibility during Hurricane Harvey through coupling of observed road closures, flood modeling, and network analysis. Furthermore, by analyzing network disruptions at the census block group level, the correlation between impact severity and social demographics of the

[§] These authors contributed equally to this work.
[1] Graduate Research Assistant, Department of Civil and Environmental Engineering, Princeton University, E-Quad Princeton NJ 08540. E-mail: agori@princeton.edu (corresponding author)
[2] Post-Doctoral Fellow, Department of Civil and Environmental Engineering, Rice University, 6100 Main St., Houston, TX 77005 E-mail: ioannis.gidaris@rice.edu
[3] Professor, Department of Sociology, Rice University, 6100 Main St., Houston, TX 77005 E-mail: James.R.Elliott@rice.edu
[4] Associate Professor, Department of Civil and Environmental Engineering, Rice University, 6100 Main St., Houston, TX 77005. E-mail: jamie.padgett@rice.edu
[5] Post-Doctoral Fellow, Department of Sociology, Rice University, 6100 Main St., Houston, TX 77005 E-mail: k.loughran@rice.edu
[6] Professor, Department of Civil and Environmental Engineering, Rice University, 6100 Main St., Houston, TX 77005 E-mail: bedient@rice.edu
[7] Graduate Research Assistant, Department of Civil and Environmental Engineering, Rice University, 6100 Main St., Houston, TX 77005. E-mail: Pranavesh@rice.edu
[8] Post-Doctoral Fellow, Department of Civil and Environmental Engineering, Rice University, 6100 Main St., Houston, TX 77005 E-mail: andrew.juan@rice.edu

affected areas is investigated. This analysis is conducted for two highly populated watersheds within the city of Houston, which have contrasting flood management infrastructure and represent a broad range of demographic groups. This analysis advances understanding of the interactions between flood extent and duration, infrastructure impacts, and community vulnerability by (i) assessing the evolution of network accessibility between emergency service locations and flood-impacted areas, (ii) estimating the flood-induced increase of the emergency response travel times of the aforementioned origin-destination pairs, and (iii) highlighting potential correlations between physical and social vulnerability.

Author keywords: road network; accessibility analysis; fluvial flood modeling; urban flooding; social vulnerability; hurricane Harvey; recovery; emergency response;

Introduction

Harvey made landfall as a category 4 hurricane along the southern Texas coast on the evening of August 25, 2017. The storm moved slowly inland, stalling for nearly four days before moving back into the Gulf of Mexico and ultimately making a second landfall as a tropical storm in Louisiana. As Harvey stalled over central Texas from August 25th-30th, it unleashed an unprecedented amount of rainfall over the greater Houston region, which caused catastrophic flooding. In particular, all 22 of the major bayous in the Houston region overtopped their banks during Harvey (Lindner and Fitzgerald 2018), and this extreme riverine flooding caused widespread and prolonged impacts to the entire region.

Harvey's extreme rainfall resulted in cascading impacts (Pescaroli and Alexander 2015) to the Houston region, since widespread flooding resulted in severe transportation disruption, and ultimately caused thousands of people to become stranded without access to emergency response services or medical facilities. In total, over 60,000 residents had to be rescued across the county, according to the Harris County Flood Control District (Lindner and Fitzgerald 2018). Hurricane

Harvey was a notable extreme event because it demonstrated that secondary impacts of flooding [i.e., those that occur due to the presence of flooding (e.g., transportation network disruption) but not due to direct contact with flood waters (Arkell and Darch 2006)] can be as important as direct flood impacts (e.g., physical damage to structures). In addition to highlighting the vulnerability of the roadway network to severe disruption, this event also demonstrated the vulnerability of communities to becoming stranded or isolated during extreme events. Given that many climate scientists believe the frequency of extreme precipitation events like Hurricane Harvey is increasing (Emanuel 2017; van Oldenborgh et al. 2017), it is necessary to understand how this storm event impacted transportation infrastructure across the Houston region. Furthermore, posing a viable framework to integrate and synthesize data from various sources to uncover fluvial flood impacts on roadway networks and their dependent citizens can have far reaching benefits in supporting risk mitigation, climate adaptation and resilience planning across many hazard susceptible regions.

Specifically, there is a need to thoroughly investigate the time evolution of Harvey's impacts on the roadway network and subsequent impacts on emergency response accessibility of different Houston neighborhoods in order to identify physically vulnerable regions of the city during extreme precipitation events. Additionally, it is crucial to understand the characteristics of the communities most heavily impacted by transportation disruption in order to determine the relationship between extreme flooding, infrastructure performance, and societal impacts. Although real-time road condition data is available for major highways through the Texas Department of Transportation (TxDOT), there is little information about the status of local roads during flood events. To understand flood impacts on local transportation networks, hydrologic and hydraulic models can simulate flood evolution and identify flooded roads.

Previous studies have demonstrated the usefulness of hydrologic and hydraulic models for predicting roadway inundation/inaccessibility during flood events. Yin et al. (2017) developed future 100-yr and 500-yr coastal flooding scenarios and conducted road network analysis to determine the impact to emergency response services. Coles et al. (2017) coupled hydrodynamic flood modeling with network analysis to evaluate the impacts of two historical flood events on emergency response services in the city of York, UK. Findings from this study highlight the vulnerability of the transportation system to widespread disruption due to flood events. Green et al. (2017) compared the impacts to transportation accessibility from fluvial flooding vs pluvial events. These studies focused on road network accessibility assessment in a “static” way considering only the maximum inundation depths of the flood scenarios examined, rather than capturing the network disruption evolution and the subsequent recovery throughout the duration of an extreme flood event. Additionally, previous studies have not thoroughly investigated the demographics of impacted areas, which can be crucial in understanding how transportation disruption interacts with social vulnerability.

The objective of this paper is to quantify the evolving level of flood-induced road network disruption, with a particular focus on emergency response routes of two case study areas within Houston’s transportation system, throughout the duration of Hurricane Harvey’s rainfall. Specifically, this paper investigates how extreme fluvial flooding can result in spatially varied road network disruptions that evolve in time, which ultimately impacts access to neighborhoods across the city. This is achieved through development of a methodology that integrates observed road closure data, floodplain simulation-based estimation of road operability using advanced hydrologic/hydraulic modeling, and network accessibility analysis. The proposed methodology supports the network performance assessment of emergency response routes through evaluation of appropriate metrics developed in this study that quantify the transportation disruption between fire stations/hospitals and different neighborhoods across the city. Furthermore, indicators of social vulnerability of the communities located in the two case study areas are collected and the results of the transportation infrastructure and social vulnerability assessments are combined to explore potential correlations between areas of high physical vulnerability and high social vulnerability, and ultimately provide insights about the populations that were most severely impacted during the storm.

In the next section the two case study areas are introduced and described. The paper then continues with a detailed description of the network accessibility assessment methodology and its coupling with social vulnerability analysis, as well as the various methods, models and datasets used. Results are presented and accompanied by corresponding discussions in the subsequent section. Finally, the last section provides the conclusions and recommendations for future work within the context of transportation infrastructure resilience and emergency response planning during extreme rain events.

Case study area(s)

The two case study watersheds examined in this study are Brays Bayou and Greens Bayou, chosen because they are both highly urbanized and flood prone. Additionally, they feature contrasting riverine management infrastructure since one is concrete-lined (highly engineered) while the other is more natural, incorporating natural meanders in the channel and vegetation along/within the stream. Finally, these watersheds represent a range of demographic groups with respect to race, income, and age distribution. Two drainage basins within the city are chosen as the case study areas because this study focuses on simulating riverine-based flooding, and the boundaries of the watersheds delineate the areas that could be impacted by river flooding.

Study Area 1: Brays Bayou

The Brays Bayou watershed is located in southwest Houston (Fig. 1), featuring over 95% developed land and a population of 717,198 people. The watershed encompasses a drainage area of 332 km^2, and has over 195 km of open channels (HCFCD 2018a). The majority of the watershed, especially the central and eastern portions, is occupied by high intensity residential and commercial land uses, and across the watershed very little green space has been preserved. Brays Bayou serves as the primary drainage conduit for the watershed, flowing west to east, and the majority of the stream is channelized and lined with concrete to facilitate faster drainage during rain events. Although almost $500 million has recently been spent on watershed improvements to increase conveyance and storage during extreme rain events (HCFCD 2004), parts of the watershed remain highly vulnerable to riverine flooding (Bass et al. 2016). Flooding impacts along Brays Bayou are often exacerbated due to development patterns within the watershed, which have left little buffer space between the banks of the bayou and roads/structures.

Study Area 2: Greens Bayou

The Greens Bayou watershed is located in northeast Houston (Fig. 1), and is also highly developed with a population of 528,720 people (HCFCD 2018b). The drainage area of Greens Bayou watershed is 549 km^2, which is substantially larger than Brays Bayou, and the watershed has 496 km of open streams (HCFCD 2018b). Although the majority of the watershed is composed of residential and commercial development, there is a significant amount of forest and wetland areas in the northeast portion of the watershed. Greens Bayou and Halls Bayou are the two main tributaries within the watershed, flowing northwest to southeast, and ultimately joining in the southern portion of the watershed before flowing into the Houston Ship Channel. Both Halls and Greens Bayous are mostly natural channels, featuring large meanders and vegetation lining the banks, and consequently they drain more slowly than Brays Bayou. Although there have been a few regional detention projects completed recently in the Greens Bayou watershed (HCFCD 2018b), it has not benefited from as many flood mitigation projects and investments compared to the Brays Bayou watershed.

Methods

Overview

This study assesses the evolution of road network accessibility related to emergency response services, such as access from fire stations and hospitals to different neighborhoods in the two case study areas during Hurricane Harvey. This is accomplished through a methodology that couples fluvial flood simulation using hydrologic and hydraulic modeling with network analysis. At the core of this approach is a proposed hybrid procedure for identifying the network's road link closures during various time instants of the storm that integrates observed highway service operability data (TxDOT 2017) with simulation-based estimation of the operability of local roads based on the output of hydrologic and hydraulic models. This hybrid procedure is developed here to overcome the absence of observed data regarding the local road conditions during Hurricane Harvey. The goal of this study is to quantify the impact of flooding on the performance of the transportation system, and as such this analysis does not incorporate traffic congestion modeling. Incorporating a congestion model may provide more accurate representations of the absolute travel times associated with reaching various neighborhoods, and additional uncertain factors also deserve attention such as emergency response and driving behavior in hazardous conditions. Overall, however, this analysis seeks to isolate the impact of flooding and offers relative measures that shed light on the spatial and temporal evolution of access during flooding.

Fig. 2 presents a flowchart of the methodology developed in this study. According to this methodology, the floodplains of the case study areas are simulated using hydrologic and hydraulic analysis for various time instants of the storm. The next step corresponds to identifying the local roads of the networks that are classified as not operable due to flooding based on the simulated inundation maps. This classification is performed by establishing an inundation depth threshold η, and based on intersection of roadways and inundation depths greater than η, road segments are considered to be closed and are removed from the road network during the network analysis. Threshold η is set equal to 61 cm (~ 2 ft) (Anarde et al. 2017) following guidelines from the National Weather Service (NWS 2018) regarding the approximate water depth at which most vehicles become buoyant during flood conditions. It is noted here that lower roadway inundation depth thresholds indicating unsafe conditions for vehicles have been proposed in the literature (Coles et al. 2017; Green et al. 2017; Yin et al. 2016); however since the network accessibility performance is focused here on emergency response services and emergency vehicles are in general able to tolerate higher inundation depths (Yin et al. 2017), the higher threshold of 61 cm was chosen. However, the threshold adopted should reflect the safe traversing height for the emergency response vehicles used, and a lower threshold may be appropriate depending on the vehicle type. After the operability conditions of the network links corresponding to the local (i.e., not highways) roads are determined, this simulation-based data is integrated with similar roadway closure information that was observed for Houston's highway system for the same time instants of the storm that the simulation-based data was captured. The latter observed data was obtained by digitizing closures reported during the course of the storm by the Texas Department of Transportation (TxDOT) through their online highway condition website (TxDOT 2017). It is noted here that although the TxDOT online highway condition website provides closure data verified by TxDOT employees as well as crowd sourced data, only the former type of data was used in this study. The next step of the proposed methodology entails coupling of the hybrid simulation and observed road closure data with network accessibility analysis for the road networks of the two case study areas to ultimately (i) assess the evolution of road network accessibility between emergency response service locations and flood-impacted areas, and (ii) estimate the emergency response travel times of the aforementioned origin-destination pairs. Finally, sociodemographic data of the communities of the two case study areas are collected and processed to identify and assess social vulnerability factors of these locations, and combine them with the network accessibility performance to investigate potential correlations between social vulnerability and the storm's impact on the physical transportation infrastructure of the affected areas. More detailed discussion regarding data collection as well as description of the flood modeling, road network accessibility and social vulnerability factors involved in the methodology presented above are provided in the following subsections.

Data collection

The 2016 Southeast Texas Addressing and Referencing Map (STAR*Map) version of Houston's street centerline GIS data was obtained from the Houston-Galveston Area Council (H-GAC 2018). The locations of fire stations and hospitals corresponding to the critical emergency response facilities examined in this study were obtained from the City of Houston GIS (COHGIS) Open Data Portal (COHGIS 2018) and are shown in Fig. 1. For estimating the travel times that emergency vehicles needed to access the flood-impacted areas during Hurricane Harvey, speed limits for the highway road links of the network were collected from H-GAC (2018) and an average value of 88.5 km/h (55 mph) was used, whereas for the local road links a value of 48.2 km/h (30 mph) was assumed. To account for adverse road conditions during the storm, since it is likely that emergency vehicles could not travel at full speed, a reduction of 16 km/h (10 mph) was taken relative to the pre-storm speed limits. The latter reduced speed limits were then used as the estimated flood event speeds. Traffic signals and other driving regulations (e.g., one way streets) are not considered in the network analysis, since emergency vehicles would generally be exempt from them during a storm with the severity of Harvey. In order to assess the level of accessibility of emergency vehicles at the neighborhood scale, census block groups (BGs) were used to delineate the boundaries of each neighborhood in the two case study areas and are shown as polygons in Fig. 1. The census block groups dataset has been developed by the US Census Bureau (USCB) and was obtained from H-GAC (2018). More details about the demographic composition of the census block groups are provided in a subsequent section discussing the demographic and social vulnerability analysis.

Hydrologic and Hydraulic model

This study utilizes the hydrologic model HEC-HMS and hydraulic model HEC-RAS for modeling riverine flooding during Hurricane Harvey and estimating the inundation of local roads. Both models were developed by the US Army Corps of Engineers (USACE) and have been widely applied for flood hazard modeling including studies of the Houston region (Bass et al. 2016; Bedient et al. 2003; Ray et al. 2011). HEC-HMS simulates the rainfall-runoff process at the subbasin-scale by utilizing Green & Ampt infiltration and the Clark TC&R method for subbasin surface runoff (HEC 2010). Next Generation Weather Radar (NEXRAD) rainfall data was obtained at 4 km^2 resolution and 5-min intervals, and was calibrated to local rain gauges.

This radar data was spatially averaged over each HEC-HMS subbasin and input to the model to simulate the runoff response. HEC-RAS is a hydraulic model that represents riverine systems through a series of elevation cross sections. Water depth is calculated at each cross section based on discharge data from HEC-HMS and water surface profiles are computed through linear interpolation between cross sections. Unsteady HEC-RAS simulations utilize the dynamic wave equation to route inflow hydrographs from HEC-HMS through the river system and produce time-varying water surface profiles (HEC 2016). By post-processing these profiles in ArcGIS (2016) and utilizing DEM data obtained from H-GAC (2018), floodplain maps are generated at different points in time during the storm.

The basis of the HEC-HMS and HEC-RAS models utilized in this study for both watersheds were models obtained from the Harris County Flood Control District (HCFCD), which maintains and periodically re-calibrates these models to generate official FEMA floodplain maps. The base models for the Brays Bayou watershed were updated to reflect the substantial flood reduction projects that were recently completed, and the models were previously validated in Bass et al. (2016). HEC-HMS and HEC-RAS models for both watersheds were validated against observed streamflow and observed water level hydrographs during Hurricane Harvey to ensure that they accurately reflect the current hydrologic and hydraulic response of the areas.

Fig. 3(a) shows a comparison of modeled HEC-HMS peak flow and observed peak streamflow from each USGS gauge located within the two watersheds. On Greens Bayou, all gauges agree well with the observed peak flow except the most upstream location (gauge 1). At this location the observed streamflow is significantly higher than the modeled flow during the peak of the storm. However, the flow contribution at this location has a small impact on downstream locations, and the majority of the flood impacts from Harvey did not occur near gauge 1. The other three comparison locations (gauges 2, 3, and 4) had an absolute average peak flow difference of 8.2%, indicating good model performance. In the Brays Bayou watershed, the model performed well at all comparison locations. Although model results slightly under-predict the peak at gauge 3 and slightly over-predict the peak at gauge 4, the absolute average peak flow difference across the watershed was 11.2%. Based on visual inspection of modeled and observed hydrographs, as well as the peak flow performance metrics, the authors concluded satisfactory validation of the HEC-HMS models for both watersheds.

To validate the performance of the HEC-RAS unsteady models, observed peak stage was compared to modeled peak stage at several points along the channels. Fig. 3(b) shows the locations of all the stage gauges in both watersheds and peak stage performance for both watersheds. Gauge 11 in Greens Bayou and gauge 10 in Brays Bayou were used as downstream boundary conditions for the HEC-RAS models so no comparison for this location is provided. In addition to peak stage comparisons, the entire modeled stage hydrographs were compared to observed stage hydrographs in Brays and Greens, and a subset of the gauge comparisons are shown in Fig. 4. In the Greens Bayou watershed, the modeled stage hydrographs generally match well with observed in terms of shape, timing, and peak, as indicated by Nash-Sutcliffe Efficiency (NSE) values of 0.81 and 0.92 for gauges 4 and 7, respectively. It is noted that NSE values range from $-\infty$ to 1, with values closer to 1 indicating higher model accuracy (Nash and Sutcliffe 1970). For validation it is important to consider both the peak and timing since this study evaluates the evolution of flooding impacts through time. Although the first peak of the hydrograph is over-predicted by the model, the main peak (which caused the majority of flooding impacts) is captured well. In the Brays Bayou watershed, the modeled hydrographs match closely to the observed stage at all points during the storm, and this is confirmed by high NSE values of 0.94 and 0.93 at gauges 2 and 6, respectively.

Road network accessibility analysis

Quantification and assessment of emergency response accessibility of the case study areas is performed through network analysis (Newman 2010). First the road networks with all their links and nodes are constructed in ArcGIS. The network links represent highway and local road segments, as shown in Fig. 1. Since it is not possible to represent every road within the case study area in the network analysis (due to computational costs), the authors select main thoroughfares, based on their designation by TXDOT. The limitation of this approach is that smaller residential roads that experienced disruption during the storm are not captured. However, since emergency vehicles would likely traverse through main thoroughfares, the authors believe this approach is appropriate. The network nodes are placed at the following locations: road intersections where two or more road segments meet, the locations of fire stations and hospitals (depicted in Fig. 1), and the centroids of census block groups (which represent neighborhood-scale accessibility). Table 1 reports the road network details for the two case study areas. It should be noted that hospitals or fire stations located outside but close to each of the study areas are still included in the network analysis, since these facilities could still service neighborhoods within the study areas.

After the road network is mapped in ArcGIS, its *edge list* (Newman 2010) corresponding to a list of the all the network's links as well as the nodes that are connected is extracted such that the network is mathematically represented and appropriate network analysis algorithms are implemented. This mathematical representation is performed using network theory concepts (Newman 2010), and in particular by representing the topology of a network as a graph G =

(V,E), where $V = \{v_1, \ldots, v_n\}$ and $E = \{e_1, \ldots, e_n\}$ are sets of n nodes and m links, respectively. Any graph G with n nodes can then be represented by its nxn *adjacency matrix* **A**, where $A_{ij} = 1$ if there is a link directly connecting v_i to v_j ($i \neq j$) and $A_{ij} = 0$ otherwise (Newman 2010; Zuev et al. 2015). The concept of an adjacency matrix is illustrated in Fig. 5(a) through a simple graph as an example representing a network under normal conditions that has not sustained any disruptions yet. Fig. 5(b) presents how the adjacency matrix is modified for a network that is disrupted because various road links are not operable due to flooding conditions. It is noted that identification of these non-operable road links is performed through the hybrid methodology described in the previous section.

The previous mathematical representation of a network is binary, i.e., the links form simple on/off connections between the nodes. However, in some cases it is useful to represent links as having a weight to them. Such weighted networks can be represented by giving the elements of the adjacency matrix values equal to the weights of the corresponding connections (Newman 2010). In road transportation networks it is common to use the road link length and road link travel time as weights such that quantities like shortest (i.e., minimum distance covered) and quickest (i.e., minimum travel time required) paths between two nodes of interest can be evaluated through networks analysis (Coles et al. 2017; Green et al. 2017; Yin et al. 2017). Here, these two choices are adopted as link weights w_{ij}, with the link length l_{ij} calculated in ArcGIS and the travel time t_{ij} estimated as $t_{ij} = l_{ij}/s_{ij}$, where s_{ij} denotes the estimated flood event speed for each network link ij connecting nodes v_i and v_j. Flood event speeds s_{ij} are estimated through the approach discussed in a previous section.

Finally, after the network is mathematically represented through **A** and w_{ij}, the network accessibility performance is quantified through analysis that calculates the shortest and quickest paths for a vehicle traversing from any origin node O to any destination node D of interest. These quantities are calculated by solving the *shortest-path problem* (Pollack and Wiebenson 1960) using Dijkstra's algorithm (Dijkstra 1959) with weights w_{ij} equal to l_{ij} and t_{ij} for the determination shortest and quickest path, respectively. Then, the network's accessibility performance is assessed by evaluating the following two metrics:

(i) *Travel time increase* $T_{O\rightarrow D}^{incr}$ corresponding to the increase in travel time for traversing along the OD pair on the disrupted road network. In particular $T_{O\rightarrow D}^{incr}$ is calculated as

$$T_{O\rightarrow D}^{incr} = T_{O\rightarrow D}^{flood} - T_{O\rightarrow D}^{undisrupted} \quad (1)$$

where $T_{O\rightarrow D}^{undisrupted}$ and $T_{O\rightarrow D}^{flood}$ denote the *minimum travel time* needed for traversing along OD pair for the undisrupted and the flood-induced disrupted road network, respectively. The minimum travel time is calculated by summing the weights $w_{ij} = t_{ij}$ of the road links comprising the quickest path between O and D.

(ii) *Connectivity loss* $CL_{O\rightarrow D}$ corresponds to a measure of the efficiency reduction when traversing along an OD pair on the disrupted road network. In particular, $CL_{O\rightarrow D}$ is mathematically expressed as

$$CL_{O\rightarrow D} = 1 - \frac{L_{O\rightarrow D}^{undisrupted}}{L_{O\rightarrow D}^{flood}};\ 0 \leq CL_{O\rightarrow D} \leq 1 \quad (2)$$

where $L_{O\rightarrow D}^{undisrupted}$ and $L_{O\rightarrow D}^{flood}$ denote the lengths of the shortest OD path for the undisrupted and the flood induced disrupted road network, respectively. The metric $CL_{O\rightarrow D}$ is a continuous variable that takes values between 0 and 1, with $CL_{O\rightarrow D}$ = 0 corresponding to the case that there is no connectivity loss between the OD pair of interest (i.e., the accessibility of the OD pair is not affected at all by the flooding conditions in the area), whereas $CL_{O \rightarrow D} = 1$ corresponds to *complete* connectivity loss for this OD pair (i.e., the flooding conditions in the area do not allow vehicles to travel from O to D).

Demographic and Social Vulnerability Analysis

For the present study, social vulnerability is conceptualized as a function of two broad dynamics: production and distribution (Tierney 2014). The social *production* of vulnerability is operationalized as the construction of residences in places with greater exposure to transportation disruption during extreme urban flooding. Such exposure can derive from pre-existing conditions, such as location in a floodplain, from nearby development that increases runoff into the area, from increased rainfall, or from a combination of all three. The social *distribution* of vulnerability is operationalized as the unequal spread of transportation disruption across different residential subpopulations, especially those who have less social privilege or need additional assistance in times of emergency. Because housing in the United States is allocated through a market system, the burdens of such inequality often fall disproportionately on lower income residents; and because this market system is embedded within a highly racialized society, people of color tend to be hit especially hard. These conditions are salient in Houston, with its long history of Jim Crow segregation and current status as one of the most economically unequal and racially segregated metropolitan areas in the United States (Emerson et al. 2012), in addition to having well documented types of environmental injustice (Bullard 1990; Elliott and Smiley 2017; Hernandez et al. 2015).

To measure both the social production and distribution of vulnerability, block-group level data are drawn from the 2016 American Community Survey (5-Year Sample). Block groups (BGs) are the smallest unit of geography for most census data due to confidentiality restrictions and typically range from 600 to 3,000 residents. Measures of the production of vulnerability focus on the number of existing housing units built in each decade following federal institutionalization of the National Flood Insurance Program (NFIP) in 1968, which collects and spends billions of dollars each year to subsidize development in flood-prone areas. For these variables, aggregate counts rather than proportions are used because areas with more aggregate housing development have higher absolute risk of disruption.

By contrast, measures of the distribution of vulnerability use averages and proportions because when it comes to disparate impacts, the social composition of an area is more important than its aggregate size. In this way, block groups with higher shares of less privileged or otherwise vulnerable residents, but relatively small populations, can still be more at risk. Here, primary attention focuses on the median household income and racial composition of block groups because class and race remain overwhelmingly powerful determinants of residential location in the United States. In addition, indicators are also included for the proportions of younger residents (under 14), older residents (over 64), those receiving public assistance, and those living in households with no vehicle with which to evacuate. These additional variables are common indicators of subpopulations needing more assistance in times of disaster (Cutter et al. 2003).

In analyses below, the correlation of each census variable with road network accessibility loss is assessed independently and net of one another using standard regression techniques (e.g. linear least squares regression). This approach maximizes transparency and minimizes concerns about appropriate weighting among respective indicators, which is a common concern in social vulnerability research relying on multi-item factor analysis (Rygel et al. 2006).

Results and Discussions

Road network accessibility performance assessment

The road network accessibility performance assessment of the two case study areas is conducted by solving the shortest-path problem using Dijkstra's algorithm in MATLAB (MathWorks 2018) for various origin-destination (OD) paths of interest to ultimately evaluate the accessibility metrics described previously. To assess the overall accessibility performance of the road networks of the two study areas during the evolution of Hurricane Harvey, the following ratios are calculated: (i) $r_1 = N^1_{OD,operable} / N^1_{OD}$ and (ii) $r_2 = N^2_{OD,operable} / N^2_{OD}$, where $N^1_{OD,operable}$ denotes the number of all possible OD paths in the entire road network that are operable (i.e., there exists a set of road links in the network such that a vehicle starting from node O can reach node D) and N^1_{OD} denotes the number of all possible OD paths (operable or not) in the road network. The quantities $N^2_{OD,operable}$ and N^2_{OD} are defined similarly to $N^1_{OD,operable}$ and N^1_{OD}, with the exception that they correspond to a subset of the road network in the vicinity (~ 1 mile from each bayou bank) of the bayou streams. Fig. 6 compares the evolution during the Harvey of the ratios r_1 [part (a)] and r_2 [part (b)] between the two case study areas.

The recovery curves shown in Fig. 6 facilitate visualization of how the entire transportation network is impacted throughout the duration of Harvey. Across the watershed [Fig. 6(a)], Greens Bayou experiences more severe impacts in terms of reduction in number of operable routes compared to Brays Bayou. In addition, the road network in Brays Bayou recovers more quickly than in Greens Bayou, and the network reaches 95% operability by the evening of August 27th. In contrast, it takes two more days (until August 29th) before the network in Greens Bayou watershed reaches comparable operability. For neighborhoods within 1 mile of the bayou banks [Fig. 6(b)], both Greens and Brays experience similar magnitudes of operability loss. This is because during the peak of the storm there was substantial riverine flooding in both watersheds, which inundated the majority of roads near the bayous. However, the impacts in Greens Bayou last much longer than in Brays Bayou, demonstrating that while the magnitude of impact is comparable between watersheds, the duration of impact is much more severe in Greens Bayou. The latter behavior in the recovery pattern of the two watersheds is attributed to the different channel characteristics between the two watersheds. In particular, Brays Bayou is a concrete-lined channel that drains relatively quickly, which allows floodwaters to subside and drain from the streets more quickly. On the other hand, Greens is a natural channel that drains much more slowly than Brays, resulting in prolonged impacts to the transportation network during Harvey. Although natural channels are often able to better attenuate a flood wave during storm events compared to concrete-lined channels due to higher friction with the channel bed (Jacobson et al. 2015; Sholtes and Doyle 2010), these higher frictional forces also result in slower drainage.

Fig. 7 illustrates the average connectivity loss between all fire stations in the watershed and each census block group for three different points in the storm: August 27 5:00 am, August 27 5:00pm, and August 28 6:00pm. Blue represents areas of low connectivity loss (high accessibility), while yellow represents moderate loss, and red represents complete connectivity loss (no accessibility). The average connectivity loss at each block group for each point in time considers the connectivity loss between each fire station in the area and the specific block group. This value is calculated using Eq. (3):

$$\overline{CL}_{F\rightarrow BG} = \frac{1}{n_F}\sum_{i=1}^{n_F} CL_{F(i)\rightarrow BG} \tag{3}$$

where $\overline{CL}_{F\rightarrow BG}$ is the average connectivity loss across all n_F fire stations for a specific block group, and $CL_{F(i)\rightarrow BG}$ is the connectivity loss between the i^{th} fire station and a specific census block group. Although constraints could be imposed that restrict the allocation of the fire stations' resources (i.e., rescue crews, emergency response vehicles, etc.) only to the census block groups within each fire station's district jurisdiction, for the purpose of this study it is assumed that in broad scale emergency situations, like Hurricane Harvey, cross-jurisdictional sharing of resources is taking place. Therefore, the idealized composite metric $\overline{CL}_{F\rightarrow BG}$ is used such that the overall level of emergency response accessibility performance across all fire stations and each census block group is captured.

During the first two time instants there is significant connectivity loss in both Brays Bayou and Greens Bayou, with numerous areas completely inaccessible from any fire station. In general, high connectivity loss areas are clustered along the bayous in both watersheds, since this is where flooding is the most severe. Connectivity loss decreases, and accessibility increases, moving away from the bayou. However, in the Brays watershed there are a few high loss areas that are located far from the bayou. These areas became inaccessible because of flooding of major highways adjacent to the neighborhoods. At each point in time during the storm, areas of high connectivity loss correlate with the location of the flood wave within the bayou. For example, Greens and Halls Bayous drain from northwest to southeast, so areas of high connectivity loss are also seen to shift from northwest to southeast as time progresses. Similarly, Brays bayou drains from west to east, so areas of high connectivity loss are more prevalent on the western side of the watershed during the beginning of the storm, and areas of high loss are prevalent on the east side of the watershed later in the storm. By August 28th 6:00pm, the majority of census block groups in Brays Bayou have restored accessibility. In contrast, Greens

Bayou still experiences high connectivity loss in some parts of the watershed on August 28th 6:00pm. This behavior is a result of the different channel characteristics between the two bayous that lead to different watershed responses and consequently to different recovery patterns as indicated in Fig. 6.

Similarly to Eq. (3) the average connectivity loss between hospitals and census block groups is expressed as:

$$\overline{CL}_{H \to BG} = \frac{1}{n_H} \sum_{k=1}^{n_H} CL_{H(k) \to BG} \tag{4}$$

where $\overline{CL}_{H \to BG}$ is the average connectivity loss across all n_H hospitals for a specific block group, and $CL_{H(k) \to BG}$ is the connectivity loss between the k^{th} hospital and a specific census block group.

Fig. 8 depicts similar results as Fig. 7 for $\overline{CL}_{H \to BG}$. The patterns of high connectivity loss areas are similar between Fig. 7 and Fig. 8, and the accessibility evolution through time is also similar. However, Fig. 8 demonstrates that the location of emergency services relative to different areas of the watershed can also have a substantial impact on block group connectivity loss. For example, in the Greens Bayou watershed, the locations of hospitals are clustered in the southwest region. In order for medical teams to reach block groups on the northeast side of the watershed, they must cross over the bayou. Since many roads near the bayou are inaccessible, this results in overall higher connectivity loss for block groups on the northeast side. Fig. 8(d) and Fig. 8(e) show more yellow and orange block groups compared to Fig. 7(d) and Fig. 7(e), indicating that these areas are more difficult to access from hospitals compared to fire stations. In Brays Bayou, there are a greater number of hospitals and they are more evenly distributed across the watershed, so this impact is not observed.

Fig. 9 illustrates the time increase (in minutes) for traversing between fire stations in the watershed and each census block group compared to undisrupted network conditions calculated using Eq. (1) for three different points in the storm: August 27 5:00 am, August 27 5:00pm, and August 28 6:00pm. Blue represents areas of low time increase (high accessibility), yellow represents moderate time increase, red represents high time increase (low accessibility), and the gray hatched areas represent census block groups that they are not accessible at all ($CL_{F\rightarrow BG}$ =1.0). It should be noted that the minimum travel time $T_{F\rightarrow BG}^{undisrupted}$ between fire stations and census block groups corresponding to undisrupted network conditions is calculated using the reduced speed limits (discussed in Methods section). Such selection aims to isolate and highlight the impact of network disruption due to flood-induced road link closures on the travel time increase, while in reality higher travel time increases are likely to be exhibited because the speed limits for the pre-storm conditions would be higher. Given that the speed of emergency vehicles in non-storm conditions may also be affected by other factors, like congestion, this comparison offers a consistent basis for inferring flood related impacts. In general, a similar pattern as with the connectivity loss maps in Fig. 7 is observed in terms of the concentration of severely disrupted areas of the network along the bayous and the evolution of these areas during the storm. However, a few differences with respect to the magnitude of time increase between the two watersheds can be seen by comparing the results of the left (Brays) and right (Greens) columns of the figure. In particular, longer delays in reaching various census block groups from fire stations are exhibited in Greens Bayou compared to Brays. The reason for this result is the larger spatial extent of network disruption due to flooding conditions experienced in Greens Bayou and also demonstrated in Fig. 6(a) and Fig. 7. Similarly to Fig. 9, the time increase (in minutes) for traversing between hospitals in the watershed and each census block group compared to undisrupted network conditions is presented in Fig. 10 for the same three characteristic points in time. Comparing Fig. 9 and Fig. 10 it can be seen that although the pattern of concertation of heavily disrupted areas along the bayous and its evolution is preserved, it is interesting to observe that significantly longer delays are observed in the northern part of the Greens watershed for the entire storm evolution. The latter behavior is the result of unequal distribution of the hospital locations in the Greens watershed and it further confirms the results of Fig. 8.

In order to understand the overall accessibility loss incurred by each census block group, it is important to consider both the magnitude of loss and the duration. Since some BGs may experience high loss for a short duration while others may experience moderate loss over a prolonged period of time, it is necessary to develop a standardized connectivity loss metric that weighs the magnitude of loss by the length of time that loss is experienced. The time-weighted connectivity loss metric for hospitals $CL^{tw}_{H\to BG}$ is defined as follows:

$$CL^{tw}_{H\to BG} = \frac{\sum_{j=1}^{n_t-1} \Delta t^{j} \left(\overline{CL}^{j}_{H\to BG} + \overline{CL}^{j+1}_{H\to BG}\right)/2}{\sum_{j=1}^{n_t-1} \Delta t^{j}} \qquad (5)$$

where Δt^{j} is the time duration in hours between the j^{th} and $j^{th}+1$ point in the storm, n_t is the total number of time instants, $\overline{CL}^{j}_{H\to BG}$ and $\overline{CL}^{j+1}_{H\to BG}$ is the average connectivity loss between hospitals and census BGs at time j and $j+1$, respectively. The time-weighted connectivity loss metric for fire stations $CL^{tw}_{F\to BG}$ is defined in a similar manner by substituting $\overline{CL}^{j}_{H\to BG}$, $\overline{CL}^{j+1}_{H\to BG}$ with $\overline{CL}^{j}_{F\to BG}$, $\overline{CL}^{j+1}_{F\to BG}$.

Fig. 11 shows a map of $CL^{tw}_{F\to BG}$ between census BGs and hospitals for the Greens Bayou watershed. The map ranges from zero (no loss at any point in time), to one (complete loss at every point in time). Fig. 11 also shows a graph of the connectivity loss through time for three different census BGs that represent a range of impacts. Census BG #1 has low connectivity loss throughout the duration of the storm, indicating less severe disruption. BG #2, which is shown in green, displays moderate loss through time since it experiences high connectivity loss for a short duration. Finally, BG #3 (shown in orange) displays high loss through time since it experiences complete connectivity loss for almost an entire day during the storm. Although similar analyses were conducted for fire stations in the Greens Bayou watershed and for both hospitals and fire stations in Brays Bayou, the authors have focused on the results presented in Fig. 11 because they best highlight that the distribution of impacts across the watershed can be uneven. With the exception of a few census BGs on the southwestern side of Halls Bayou, the time-weighted connectivity loss increases with increasing distance from hospitals. This is likely because to reach census BGs in the middle of the watershed, emergency responders must cross over Halls Bayou, where a significant number of roads are inaccessible. Reaching the northwest portion of the watershed is even more difficult, since responders must cross over both Halls and Greens Bayous. Fig. 11 illustrates how the location of emergency services relative to the location of the bayous (or areas of major flooding) can combine to exacerbate transportation disruption for some areas of the watershed.

Social production and distribution of vulnerabilities to transportation disruptions

Analysis of social vulnerability starts with aggregate differences between the two areas under investigation. Model results in Table 2 indicate that during Hurricane Harvey, Greens Bayou suffered more transportation disruption than Brays Bayou, regardless of how that disruption is measured (e.g. maximum over time or time averaged connectivity loss to fire stations or hospitals). Table 2 also indicates that Greens Bayou is less socially privileged than Brays Bayou across a number of common demographic indicators. Its nonwhite population, for example, is 93% compared with 49% in Brays Bayou, and its median household income is approximately $35,000 per year compared with $82,000 per year. In addition, the relative presence of children and households receiving public assistance are also higher in Greens Bayou than in Brays Bayou. Thus, overall, findings indicate that demographically, at least, the more socially vulnerable of the two study areas experienced greater transportation disruption.

In addition, Table 2 also indicates that these differences are not monolithic; instead, substantial variation exists within each area, as well. In Brays Bayou, for example, the proportion of black residents ranges from 0% to 97% in constituent block groups. The median household income ranges from less than $15,000 to $250,000, and the proportion of households with no vehicle ranges from 0% to 43%. In Greens Bayou, even greater variation exists along these same variables. Consequently, ample opportunity exists for disparate transportation disruption within as well as across the two study areas.

To test for these more localized disparities, least squares regression equations of the following general form were estimated at the block group level to assess correlations between respective census variables and measures of transportation disruption:

$$PIV = \beta_0 + \beta_1 \left[\text{Bayou Area}\right] + \beta_{2i} \left[\text{Social Distribution}\right]_i + \beta_{3j} \left[\text{Social Production}\right]_j + \varepsilon \qquad (6)$$

where all variables are measured at the block group level: *PIV* is the respective measure of physical infrastructure vulnerability (*PIV)* in the block group corresponding to maximum over time average connectivity loss for fire stations/hospitals ($\overline{CL}_{F \to BG}$ or $\overline{CL}_{H \to BG}$) or the time-weighted connectivity loss for fire stations/hospitals ($CL^{tw}_{F \to BG}$ or $CL^{tw}_{H \to BG}$), β_0 is the intercept coefficient, β_1 is the coefficient for the mean difference in the respective *PIV* in Greens Bayou versus Brays Bayou (the reference category), which accounts for aggregate differences at the watershed-scale, β_{2i} is the vector of coefficients for the change in the respective *PIV* given a one-unit change in the i^{th} measure of social distribution (e.g., racial composition, household income, etc.), β_{3j} is the vector of coefficients for the change in the respective *PIV* given a one-unit change in j^{th} measure of social production (e.g., the number of residential units built before 1970, during the 1970s, etc.) and ε is the error term. In the multiple linear regression framework used here, all coefficients for all variables are estimated net of other variables in the model and thus indicate the marginal, or partial, contribution of that variable while statistically controlling for all other variables in the model.

Table 3 presents regression coefficients for all demographic variables considered in Eq. (6) and represents the partial correlation of each variable with the observed transportation disruption. These results are meant to highlight potential correlations between demographic indicators and physical impacts, and do not assume any causal relationship between the indicator variables and the observed transportation disruption. Overall, results in Table 3 show no sign of conventional racial inequalities; instead, the opposite appears to be the case. After controlling for baseline differences between the two study areas, block groups with higher proportions of black and Hispanic residents generally experienced lower levels of transportation disruption during Hurricane Harvey, all else equal. The same is true for households with no vehicle; the higher their proportion in a block group, the lower the transportation disruption.

Evidence of more common inequalities is strongest with respect to income, which is statistically significant for models predicting maximum disruption to and from nearby hospitals and fire stations ($p < .05$). To illustrate, Fig. 12(a) plots estimated levels of maximum over time transportation disruption from Models (1) and (2) across the full range of observed median household incomes, holding all other variables constant at their means. Here, the inverse relationship between income and disruption is easy to see. At the extremes, a block group with a median income of $30,000 per year had roughly twice the predicted transportation disruption as a block group with a median income of $250,000 (e.g., 0.43 versus 0.21 for fire stations, all else equal).

Turning next to the social production of vulnerability, results in Table 3 also show a consistent pattern. That pattern indicates that block groups heavily developed during the 1970s, soon after establishment of the National Flood Insurance Program, had the most transportation disruption during Harvey, followed by block groups with more recent development. The production of risk, in other words, seems to be taking a U-turn. Instead of new development continuing to reduce the threat of local transportation disruption, as it seems to have done during the 1980s and 90s, it has been pushing that threat upward again. To visualize this trend, Models (1) and (2) in Table 3 are used to simulate different scenarios, which are displayed in Fig. 11(b) in the form of a timeline. For each scenario, or data point, the number of housing units in the average block group is set to a constant value of 600 units, with all other variables set to their respective means. To the left-most of the graph, all 600 housing units in the simulated block group were built before 1970; for the next data point, they were all built during the 1970s; in the third, they were all built during the 1980s; and so forth. Results show how the production of vulnerability increased during the 1970s then receded during the 1980s and 90s, before then climbing again since 2000.

Overall, then, analyses of social vulnerability here indicate that forces of production and distribution both matter for local inequalities in transportation disruption. Specifically, they show that such disruption tends to be higher in lower-income areas and in areas developed more recently, relative to the 1980s and 90s. To see where these dynamics overlap most intensely, a composite vulnerability index was computed. For this index a block group's median household income, number of housing units constructed since 2000, and maximum estimated transportation disruption to hospitals during Harvey were each converted to percentile scores, based on the block group's rank across the two study areas, with income reverse-coded so that lower incomes indicate higher vulnerability. These three measures were then summed and mapped in Fig. 13 using the same scale across both areas to facilitate comparison. Here, the maps clearly show a greater number of (red) high-vulnerability block groups in Greens Bayou than in Brays Bayou, with high-vulnerability defined as having a composite score of two or higher. (For example, one way a block group could fall into the high-vulnerability category is if it scored in the 67th percentile on all three measures 0.67 * 3 = 2.01; or, say, in the 90th percentile on one measure, in the 60th percentile on another, and in 50th percentile on the third. In all cases, two of the three measures must be above the median to reach the high-vulnerability category.)

The maps in Fig. 13 also show high-vulnerability block groups tend to make a continuous band along the length of Greens Bayou, with some additional scattering along Halls Bayou to the south. In the Brays Bayou area, by contrast, there is a smaller scattering of high vulnerability block groups along the bayou as well a higher count of low-vulnerability block groups. In other words, the same factors produce different vulnerability landscapes in the two areas, with Greens Bayou defined by ongoing concentrations of recently developed low-income housing prone not only to flooding but related transportation disruption. It is noted here that the missing data values in the maps result from suppression of median household income data in 12 of the 358 block groups under study. Beginning in data year 2015, the Census Bureau applied a new methodology to the 5-year dollar-based medians that suppresses data for a geographic area if the margin of error exceeds the estimate itself.

Conclusions

This study provided a multidisciplinary, integrated framework to evaluate fluvial flood impacts on roadway accessibility to emergency services experienced by potentially socially vulnerable populations. The framework was applied to evaluate the evolution of emergency response accessibility in two areas of Houston, TX during Hurricane Harvey by integrating observed road closure data with hydrologic and hydraulic inundation modeling to ultimately conduct network analysis of Houston's roadways. Select accessibility metrics between fire stations/hospitals and neighborhoods (represented by census block groups) were quantified during various points in the storm to understand the impacts to residential populations. Finally, demographic indicators of the two study areas were utilized to investigate potential social vulnerability within the impacted populations. Although this paper has focused on a single case study event within the Houston region, the integrated approach combining road condition data from multiple sources can be applied to a variety of other hazard-prone regions. By tracking the evolution of roadway accessibility through time, this type of analysis could provide emergency responders and city planners with a valuable disaster-planning tool that goes beyond typical static floodplain maps. In particular, understanding which roads are likely to be flooded during extreme events, how inaccessibility of certain roads disrupts the overall transportation network, and the duration of disruption, can help emergency managers develop emergency routes that prioritize vulnerable areas. By further considering demographic indicators within this multidisciplinary study, crucial information about vulnerable groups can be obtained and can potentially aid in efficient emergency resource distribution both before and after a major flood event.

Results from accessibility analysis demonstrate that regions close to the bayous suffer the highest transportation disruption, but that unequal distribution of emergency service locations (such as hospitals) can also exacerbate impacts for some neighborhoods. Additionally, the hydrologic response of an area also has a significant impact on transportation disruption, since this affects the magnitude and duration of fluvial flooding. Although the increase in travel time between emergency response locations and different census block groups was minor for the majority of census block groups in the study areas, there were some neighborhoods in the Greens Bayou watershed that suffered travel time increases of 20 minutes or greater.

Results of the demographic analysis indicate that social vulnerability to flood-induced transportation disruption is both multi-scalar and multi-dimensional. In terms of scale, the lower-income, higher-minority area of Greens bayou suffered greater connectivity loss, overall, than the higher-income, lower-minority area of Brays bayou. In addition, and across these two areas, lower-income block groups experienced greater connectivity loss than higher-income block groups. Both patterns are consistent with prior research indicating that the impacts of disaster tend to increase in less socially advantaged areas. The same patterns also demonstrate how such disparities can operate at multiple, overlapping scales, that is, within as well as across different areas of the same city.

There are many opportunities for future work related to this study that could focus on refining both the methodology and applicability of the analysis. For example, future work should incorporate other sources of road condition data, such as crowd-sourced information or documented emergency requests, into the integrated analysis framework. Future efforts should pursue data to support validation of travel times in emergency conditions, like the Harvey flood situation. In the context of this paper the travel times are intended to offer relative measures of access and afford correlation analyses with social vulnerability scores. Further applications of this type of framework could focus on incorporating the accessibility analysis into existing real-time flood warning systems that exist within the Houston region (Fang et al. 2011), acting as a support tool to predict road network accessibility in advance of a future storm event, and giving emergency responders information about which communities may be heavily impacted before the storm hits.

Acknowledgements

This study is based on research supported by the Rice Houston Engagement and Recovery Effort (HERE) program at Rice University, as well as the National Science Foundation under award number OISE-1545837. The authors also thank Dr. Sabarethinam Kameshwar for his collaboration in collecting the TxDOT highway closure dataset. Any opinions, findings and recommendations presented in this work are those of the authors and do not necessarily reflect the views of the sponsor.

References

Anarde, K. A., Kameshwar, S., Irza, J. N., Nittrouer, J. A., Lorenzo-Trueba, J., Padgett, J. E., Sebastian, A., and Bedient, P. B. (2017). "Impacts of Hurricane Storm Surge on Infrastructure Vulnerability for an Evolving Coastal Landscape." *Natural Hazards Review*, 19(1), 04017020.

ArcGIS, E. (2016). "10.4.1." *Redlands, California: ESRI*.

Arkell, B., and Darch, G. (2006). "Impact of Climate Change on London's Transport Network." *Proceedings of the ICE–Municipal Engineer*, 159(4), 231-237.

Bass, B., Juan, A., Gori, A., Fang, Z., and Bedient, P. (2016). "2015 Memorial Day Flood Impacts for Changing Watershed Conditions in Houston." *Natural Hazards Review*, 18(3), 05016007.

Bedient, P. B., Holder, A., Benavides, J. A., and Vieux, B. E. (2003). "Radar-based flood warning system applied to Tropical Storm Allison." *Journal of Hydrologic Engineering*, 8(6), 308-318.

Bullard, R. D. (1990). *Dumping in Dixie: Race, class, and environmental quality*, Westview Press.

COHGIS (2018). "City of Houston GIS Open Data Portal." <https://cohgis-mycity.opendata.arcgis.com/>. (June 2018).

Coles, D., Yu, D., Wilby, R. L., Green, D., and Herring, Z. (2017). "Beyond 'flood hotspots': Modelling emergency service accessibility during flooding in York, UK." *Journal of hydrology*, 546, 419-436.

Cutter, S. L., Boruff, B. J., and Shirley, W. L. (2003). "Social vulnerability to environmental hazards." *Social science quarterly*, 84(2), 242-261.

Dijkstra, E. W. (1959). "A note on two problems in connexion with graphs." *Numerische mathematik*, 1(1), 269-271.

Elliott, J. R., and Smiley, K. T. (2017). "Place, Space, and Racially Unequal Exposures to Pollution at Home and Work." *Social Currents*, 2329496517704873.

Emanuel, K. (2017). "Assessing the present and future probability of Hurricane Harvey’s rainfall." *Proceedings of the National Academy of Sciences*, 201716222.

Emerson, M. O., Bratter, J., Howell, J., Jeanty, P. W., and Cline, M. (2012). "Houston region grows more racially/ethnically diverse, with small declines in segregation." *A joint report analyzing census data from*, Kinder Institute for Urban Research, Houston, TX.

Fang, Z., Bedient, P. B., and Buzcu-Guven, B. (2011). "Long-term performance of a flood alert system and upgrade to FAS3: A Houston, Texas, case study." *Journal of Hydrologic Engineering*, 16(10), 818-828.

Green, D., Yu, D., Pattison, I., Wilby, R., Bosher, L., Patel, R., Thompson, P., Trowell, K., Draycon, J., and Halse, M. (2017). "City-scale accessibility of emergency responders operating during flood events." *Natural Hazards and Earth System Sciences*, 17(1), 1.

H-GAC (2018). "Houston-Galveston Area Council." <http://www.h-gac.com/rds/GIS_Data/starmap/default.aspx>. (June 2018).

HCFCD (2004). "Brays Bayou federak flood control project Harris County, Texas alternative to the diversion seperable element environmrntal assessment. ."

HCFCD (2018a). "Harris County Flood Control District - Brays Bayou." < https://www.hcfcd.org/projects-studies/brays-bayou/>. (June 2018).

HCFCD (2018b). "Harris County Flood Control District - Greens Bayou.", < https://www.hcfcd.org/projects-studies/greens-bayou/>. (June 2018).

HEC. 2010. Hydrologic Modeling System User’s Manual. US Army Corps Eng. 318. https://doi.org/CDP-74A.

HEC. 2016. HEC-RAS River Analysis System User ’s Manual, USACE.

Hernandez, M., Collins, T. W., and Grineski, S. E. (2015). "Immigration, mobility, and environmental injustice: A comparative study of Hispanic people’s residential decision-making and exposure to hazardous air pollutants in Greater Houston, Texas." *Geoforum*, 60, 83-94.

Jacobson, R. B., Lindner, G., and Bitner, C. (2015). "The role of floodplain restoration in mitigating flood risk, Lower Missouri River, USA." *Geomorphic Approaches to Integrated Floodplain Management of Lowland Fluvial Systems in North America and Europe*, Springer, 203-243.

Lindner, J., and Fitzgerald, S. (2018). "Immediate Report – Final Hurricane Harvey - Storm and Flood Information."Houston.

MathWorks. 2018. MATLAB Release 2018a, Inc., Natick, MA.

Nash, J. E., and Sutcliffe, J. V. (1970). "River flow forecasting through conceptual models part I—A discussion of principles." *Journal of hydrology*, 10(3), 282-290.

Newman, M. (2010). *Networks: an introduction*, Oxford university press.

NWS (2018). "National Weather Service: Turn around don't drown." <http://www.nws.noaa.gov/os/water/tadd/>. (May 2018).

Pescaroli, G., and Alexander, D. (2015). "A definition of cascading disasters and cascading effects: Going beyond the "toppling dominos" metaphor." *Planet@ Risk*, 3(1).

Pollack, M., and Wiebenson, W. (1960). "Solutions of the shortest-route problem—a review." *Operations Research*, 8(2), 224-230.

Ray, T., Stepinski, E., Sebastian, A., and Bedient, P. B. (2011). "Dynamic modeling of storm surge and inland flooding in a Texas coastal floodplain." *Journal of Hydraulic Engineering*, 137(10), 1103-1110.

Rygel, L., O'Sullivan, D., and Yarnal, B. (2006). "A method for constructing a social vulnerability index: an application to hurricane storm surges in a developed country." *Mitigation and adaptation strategies for global change*, 11(3), 741-764.

Sholtes, J. S., and Doyle, M. W. (2010). "Effect of channel restoration on flood wave attenuation." *Journal of Hydraulic Engineering*, 137(2), 196-208.

Tierney, K. (2014). *The social roots of risk: Producing disasters, promoting resilience*, Stanford University Press.

TxDOT (2017). "Drive Texas: TxDOT Highway Conditions." <https://drivetexas.org/>. (September 2017).

van Oldenborgh, G. J., van der Wiel, K., Sebastian, A., Singh, R., Arrighi, J., Otto, F., Haustein, K., Li, S., Vecchi, G., and Cullen, H. (2017). "Attribution of extreme rainfall from Hurricane Harvey, August 2017." *Environmental Research Letters*, 12(12), 124009.

Yin, J., Yu, D., Lin, N., and Wilby, R. L. (2017). "Evaluating the cascading impacts of sea level rise and coastal flooding on emergency response spatial accessibility in Lower Manhattan, New York City." *Journal of hydrology*, 555, 648-658.

Yin, J., Yu, D., Yin, Z., Liu, M., and He, Q. (2016). "Evaluating the impact and risk of pluvial flash flood on intra-urban road network: A case study in the city center of Shanghai, China." *Journal of hydrology*, 537, 138-145.

Zuev, K. M., Wu, S., and Beck, J. L. (2015). "General network reliability problem and its efficient solution by subset simulation." *Probabilistic Engineering Mechanics*, 40, 25-35.

Table 1. Details for the road networks of the two case study areas

Case Study Area	Road network links			Road network nodes				
	Highway roads	Non-highway roads	Total $m =$	Fire Stations $n_F =$	Hospitals $n_H =$	Census Block Group Centroids $n_{BG} =$	Junctions	Total $n =$
Brays	118	780	998	13	24	213	388	638
Greens	105	841	946	11	6	145	560	722

Table 2. Descriptive Statistics for Census Indicators at the Block-Group Level for the two Case Study Areas.

	Brays Bayou (n=213 block groups)		Greens Bayou (n=145 block groups)		Between-Bayou Difference (* $p < .05$)
	Mean	[Min; Max.]	Mean	[Min; Max.]	
Transportation Disruption					
Maximum over time connectivity loss					
To fire stations	0.34	[0; 1.0]	0.47	[0.20; 1.0]	*
To hospitals	0.34	[0; 1.0]	0.51	[0.25; 1.0]	*
Time-averaged connectivity loss					
To fire stations	0.08	[0.0; 0.63]	0.22	[0.10; 0.71]	*
To hospitals	0.11	[0.0; 0.62]	0.28	[0.15; 0.73]	*
Social Composition					
Race					
% black	0.19	[0.0; 0.97]	0.25	[0.0; 1.0]	
% Hispanic	0.30	[0.0; 0.98]	0.68	[0.0; 1.0]	*
% Elderly (65 years or older)	0.11	[0.0; 0.42]	0.09	[0.0; 0.47]	*
% Youth (14 years or younger)	0.20	[0.0; 0.44]	0.26	[0.04; 0.44]	*
Median household income ($x10^3)	82.4	[14.6; 250.0]	35.0	[9.4; 90.2]	*
% on Public assistance	0.01	[0.0; 0.11]	0.02	[0.0; 0.13]	*
% with No vehicle	0.08	[0.0; 0.43]	0.09	[0.0; 0.53]	
Social Production					
Number of housing units					
Built before 1970	236	[0; 701]	283	[0; 821]	*
Built during the 1970s	169	[0; 933]	154	[0; 749]	
Built during 1980s	93	[0; 835]	68	[0; 452]	*
Built during 1990s	75	[0; 813]	44	[0; 436]	*
Built since 2000	98	[0; 1134]	110	[0; 377]	
Composite Vulnerability Score[a]	1.26	[0.44; 2.32]	1.64	[0.72; 2.66]	*

[a] Construction of this vulnerability score is guided by regression findings from Table 2. For its computation, a block group's median household income, number of housing units constructed since 2000, and maximum estimated connectivity loss to hospitals during Hurricane Harvey were all converted to percentile scores, based on their rank across the two study areas and with income inverted so that lower incomes receive higher percentile scores. The three percentile measures (e.g. 0.50 for the median) were then summed. For example, if a block group scored in the 67th percentile on all three measures, its score would be 0.67 * 3 = 2.01.

Table 3. Regression coefficients (and standard errors) estimating partial correlations between socio-demographic variables and transportation disruption at the block-group level in the Brays and Greens bayou study areas.

	Maximum over time Connectivity Loss		Time-weighted Connectivity Loss	
	From fire stations	From hospitals	From fire stations	From hospitals
Model number	(1)	(2)	(3)	(4)
Bayou Area				
Brays [reference category]	---	---	---	---
Greens	.225***	.281***	.174***	.219***
	(.045)	(.044)	(.017)	(.016)
Social Distribution				
Race				
% black	-.259*	-.261**	-.087*	-.080*
	(.101)	(.099)	(.039)	(.037)
% Hispanic	-.336**	-.380**	-.091*	-.118**
	(.112)	(.111)	(.044)	(.041)
% Elderly (65 years or older)	.119	.213	-.050	-.026
	(.257)	(.253)	(.0998)	(.094)
% Youth (0-14 years old)	.087	.117	-.024	-.005
	(.218)	(.214)	(.0846)	(.0795)
Median household income ($x1000)	-.009†	-.011*	-.001	-.002
	(.004)	(.004)	(.002)	(.002)
% on Public assistance	-.529	-.481	-.089	-.091
	(.707)	(.695)	(.274)	(.258)
% with No vehicle	-.344†	-.471*	-.078	-.123†
	(.187)	(.183)	(.072)	(.068)
Social Production				
Number of housing units				
Built before 1970 [ref.]	---	---	---	---
Built during the 1970s (00)	.033**	.045***	.013**	.017***
	(.010)	(.010)	(.003)	(.003)
Built during 1980s (00)	-.001	-.0026	.0055	.003
	(.015)	(.015)	(.006)	(.005)
Built during 1990s	-.029†	-.031†	-.011†	-.011†
	(.017)	(.016)	(.006)	(.006)
Built since 2000	.012†	.010†	.009***	.008***
	(.006)	(.006)	(.002)	(.002)
Constant	.302	.252	-.052	-.064
	(.103)	(.101)	(.040)	(.037)
N	346	346	346	346
R^2	.122	.189	.354	.486

† $p < .10$; * $p < .05$; ** $p < .01$; *** $p < .001$; two-tailed test

Figure1

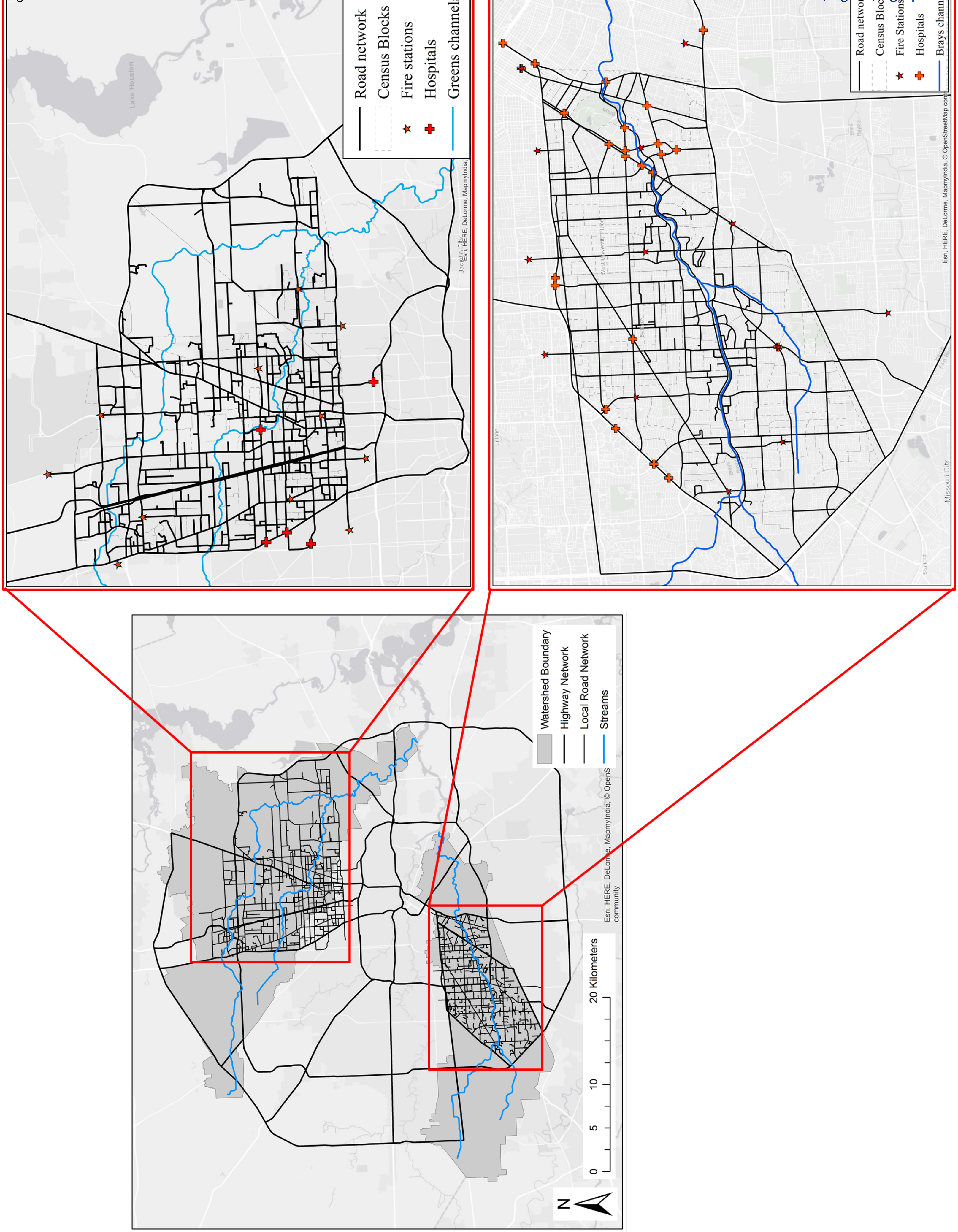
Road network
Census Blocks
Fire stations
Hospitals
Greens channels
Esri, HERE, DeLorme, MapmyIndia,
Road network
Census Blocks
Fire Stations
Hospitals
Brays channels
Esri, HERE, DeLorme, MapmyIndia, © OpenStreetMap contributors
Watershed Boundary
Highway Network
Local Road Network
Streams
Esri, HERE, DeLorme, MapmyIndia, © OpenStreetMap contributors, and the GIS user community
0
5
10
20 Kilometers
N

Figure2

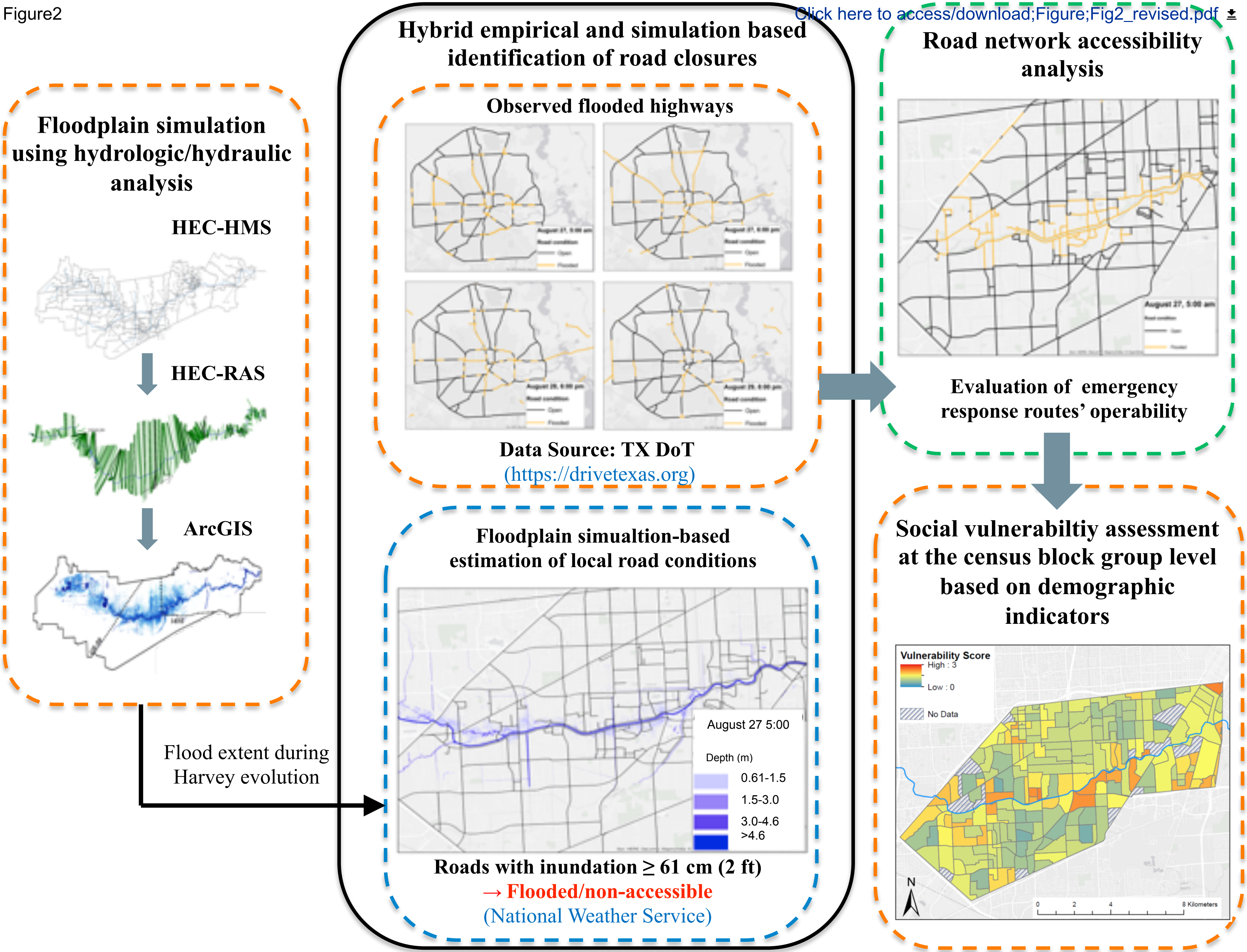

Floodplain simulation using hydrologic/hydraulic analysis
HEC-HMS
HEC-RAS
ArcGIS
Flood extent during Harvey evolution
Hybrid empirical and simulation based identification of road closures
Observed flooded highways
Data Source: TX DoT
(https://drivetexas.org)
Floodplain simualtion-based estimation of local road conditions
August 27 5:00
Depth (m)
0.61-1.5
1.5-3.0
3.0-4.6
>4.6
Roads with inundation ≥ 61 cm (2 ft)
→ Flooded/non-accessible
(National Weather Service)
Road network accessibility analysis
Evaluation of emergency response routes' operability
Social vulnerabiltiy assessment at the census block group level based on demographic indicators
Vulnerability Score
High : 3
Low : 0
No Data
N
0
2
4
8 Kilometers

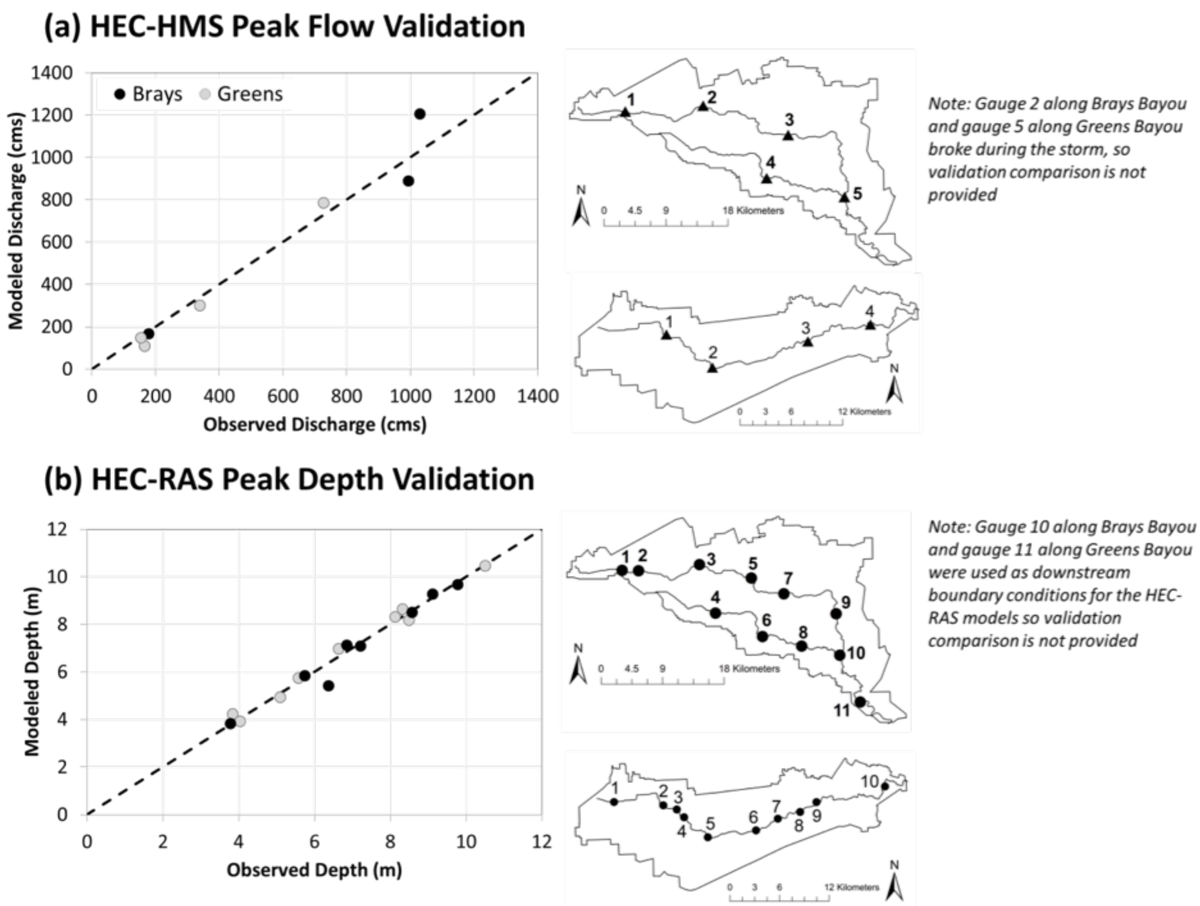
(a) HEC-HMS Peak Flow Validation
Brays
Greens
Modeled Discharge (cms)
Observed Discharge (cms)
0
200
400
600
800
1000
1200
1400
N
0
4.5
9
18 Kilometers
12 Kilometers
Note: Gauge 2 along Brays Bayou and gauge 5 along Greens Bayou broke during the storm, so validation comparison is not provided
(b) HEC-RAS Peak Depth Validation
Modeled Depth (m)
Observed Depth (m)
0
2
4
6
8
10
12
Note: Gauge 10 along Brays Bayou and gauge 11 along Greens Bayou were used as downstream boundary conditions for the HEC-RAS models so validation comparison is not provided

Figure4 Click here to access/download;Figure;Fig4.pdf

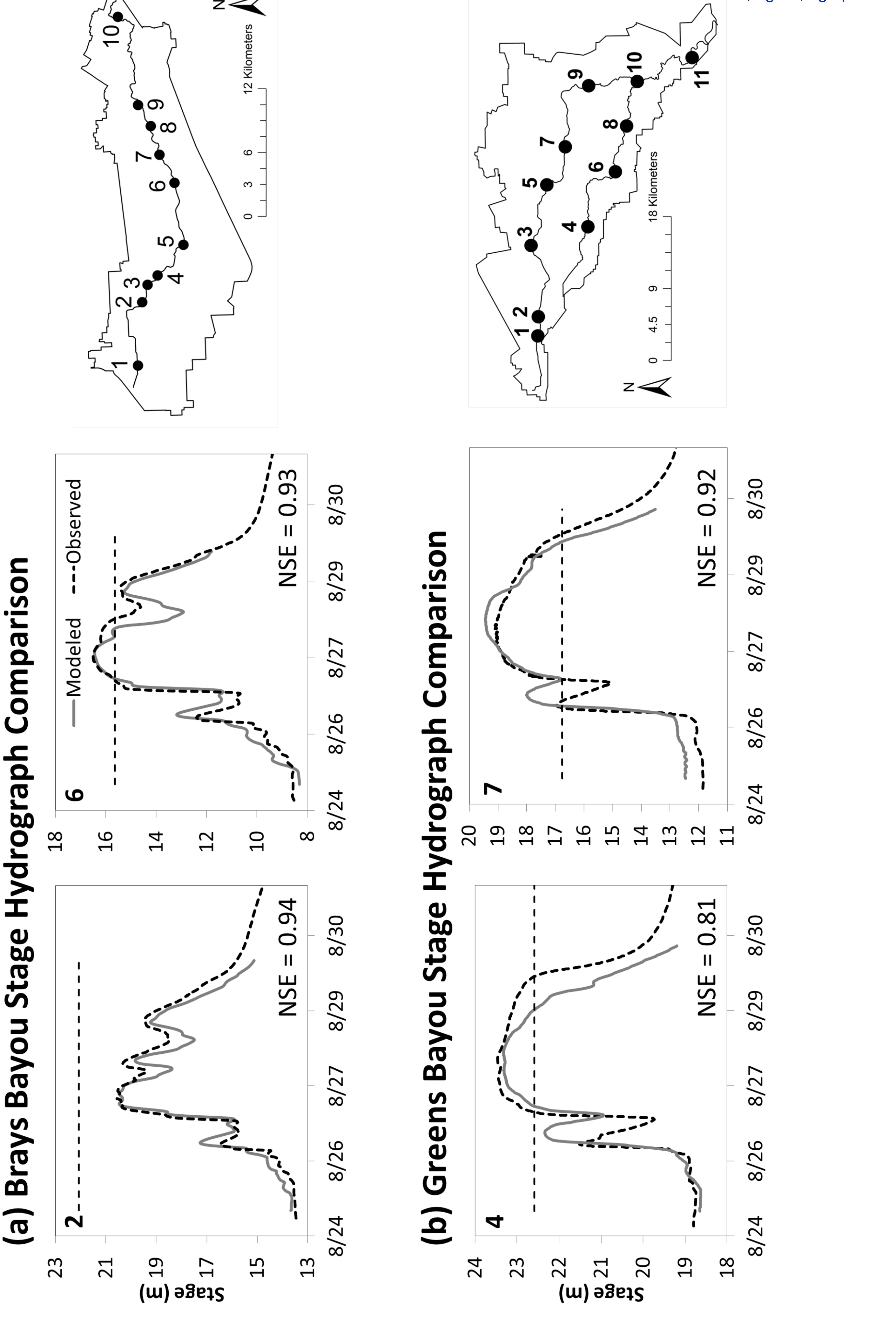

(a)

Graph

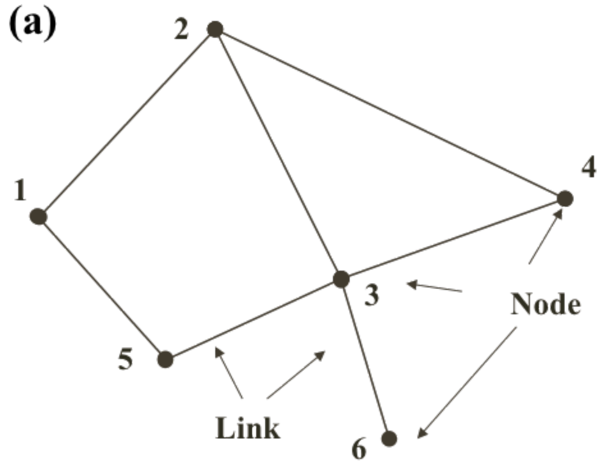

n = 6 nodes and m = 8 links

Edge list

Links (Edges)

(1,2)
(1,5)
(2,3)
(2,4)
(3,4)
(3,5)
(3,6)

Adjacency matrix

$$\mathbf{A} = \begin{bmatrix} 0 & 1 & 0 & 0 & 1 & 0 \\ 1 & 0 & 1 & 1 & 0 & 0 \\ 0 & 1 & 0 & 1 & 1 & 1 \\ 0 & 1 & 1 & 0 & 0 & 0 \\ 1 & 0 & 1 & 0 & 0 & 0 \\ 0 & 0 & 1 & 0 & 0 & 0 \end{bmatrix}$$

(b)

Graph

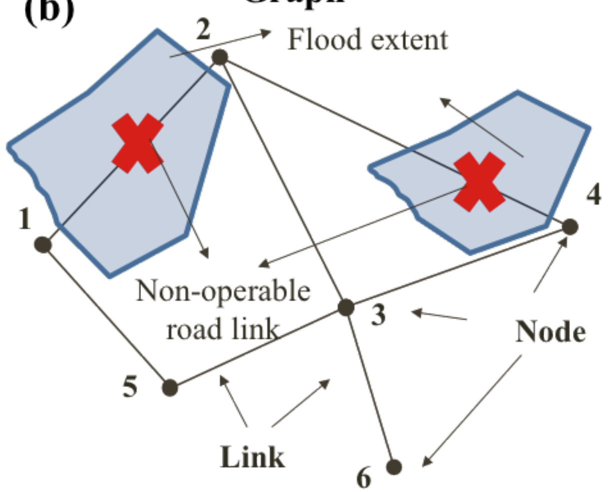

n = 6 nodes and m = 6 links

Edge list

Links (Edges)

(1,5)
(2,3)
(3,4)
(3,5)
(3,6)

Adjacency matrix

$$\mathbf{A} = \begin{bmatrix} 0 & 0 & 0 & 0 & 1 & 0 \\ 0 & 0 & 1 & 0 & 0 & 0 \\ 0 & 1 & 0 & 1 & 1 & 1 \\ 0 & 0 & 1 & 0 & 0 & 0 \\ 1 & 0 & 1 & 0 & 0 & 0 \\ 0 & 0 & 1 & 0 & 0 & 0 \end{bmatrix}$$

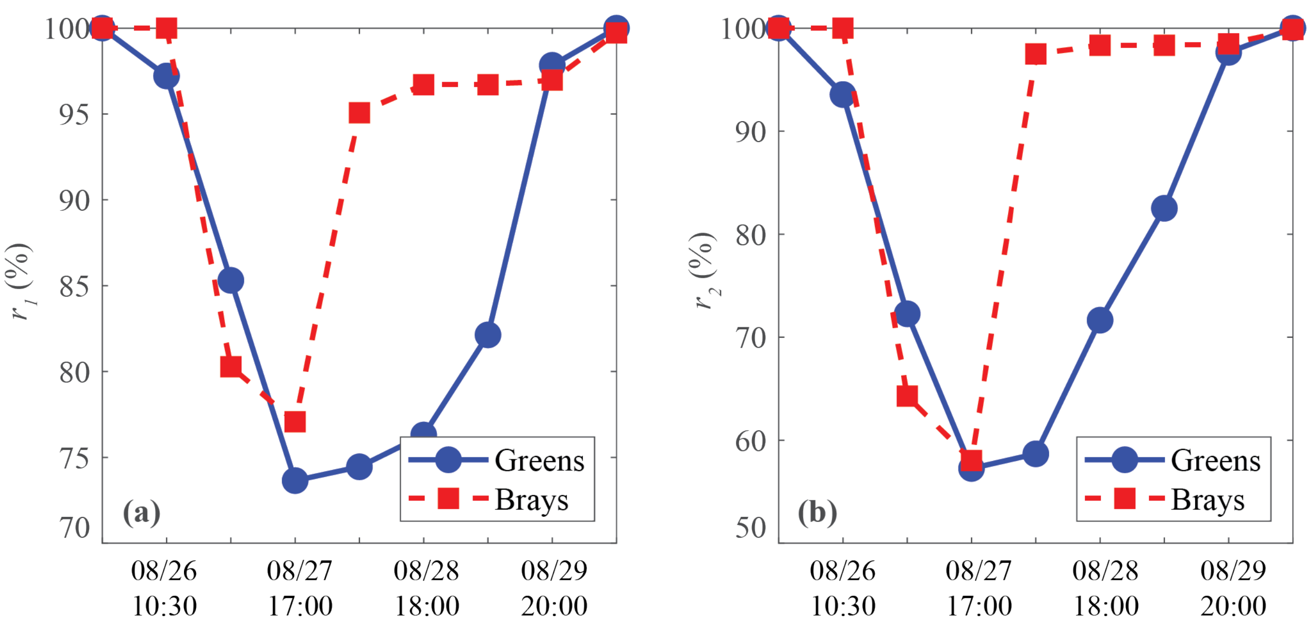
100
95
90
85
80
75
70
r_1 (%)
Greens
Brays
(a)
08/26
10:30
08/27
17:00
08/28
18:00
08/29
20:00
100
90
80
70
60
50
r_2 (%)
Greens
Brays
(b)
08/26
10:30
08/27
17:00
08/28
18:00
08/29
20:00

Figure7

Click here to access/download;Figure;Fig7.pdf

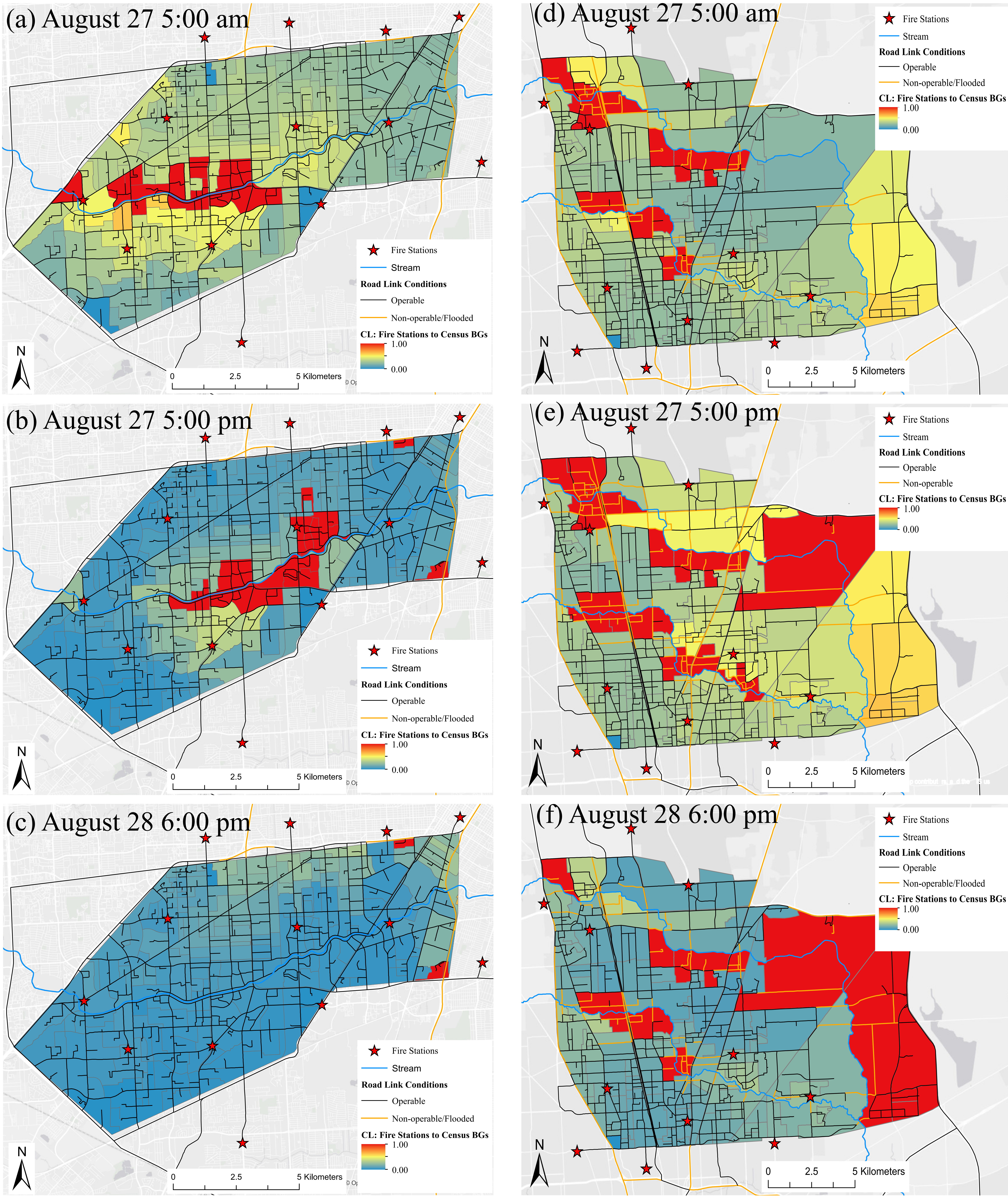

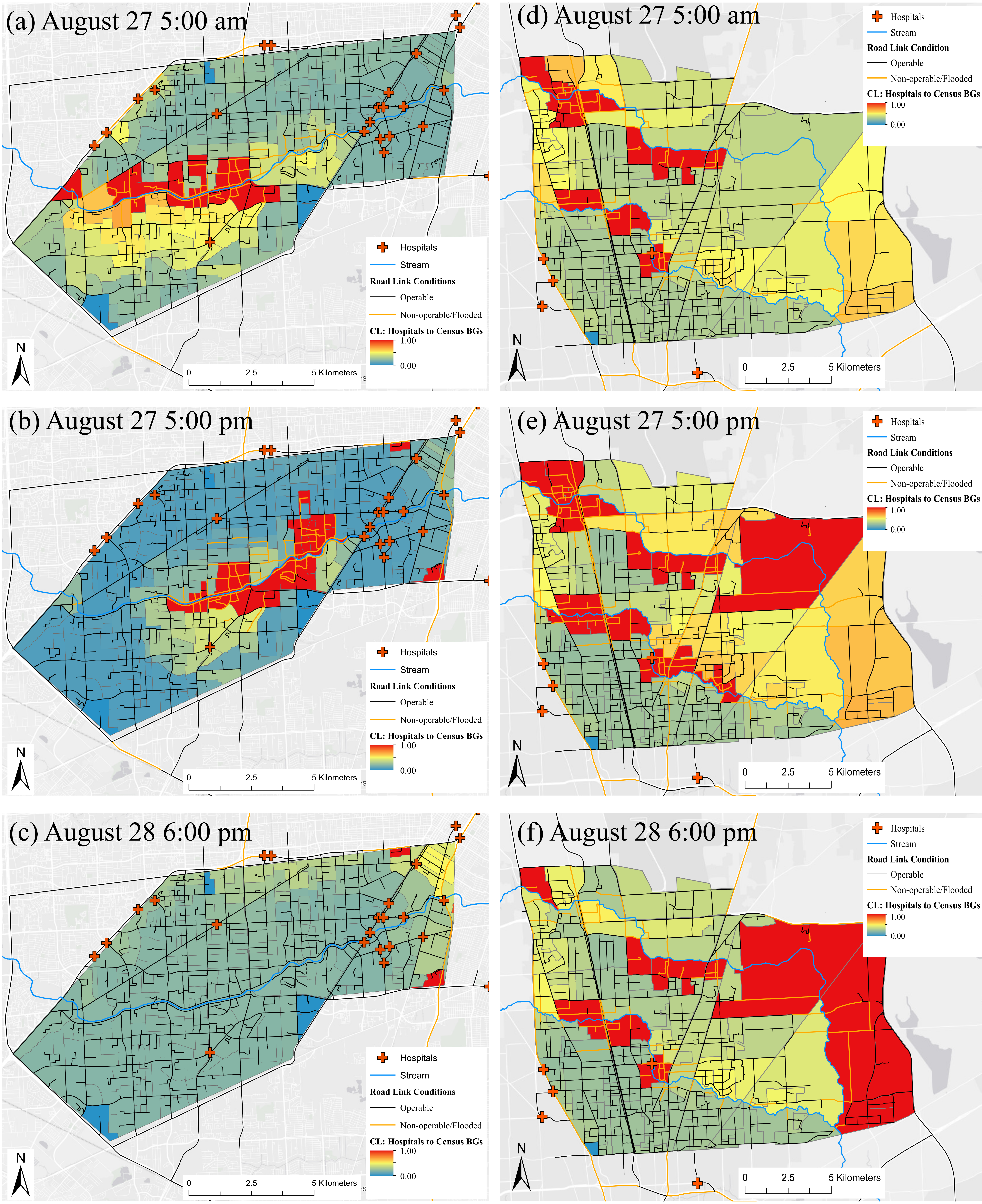
(a) August 27 5:00 am
(b) August 27 5:00 pm
(c) August 28 6:00 pm
(d) August 27 5:00 am
(e) August 27 5:00 pm
(f) August 28 6:00 pm
Hospitals
Stream
Road Link Conditions
Road Link Condition
Operable
Non-operable/Flooded
CL: Hospitals to Census BGs
1.00
0.00
N
0
2.5
5 Kilometers

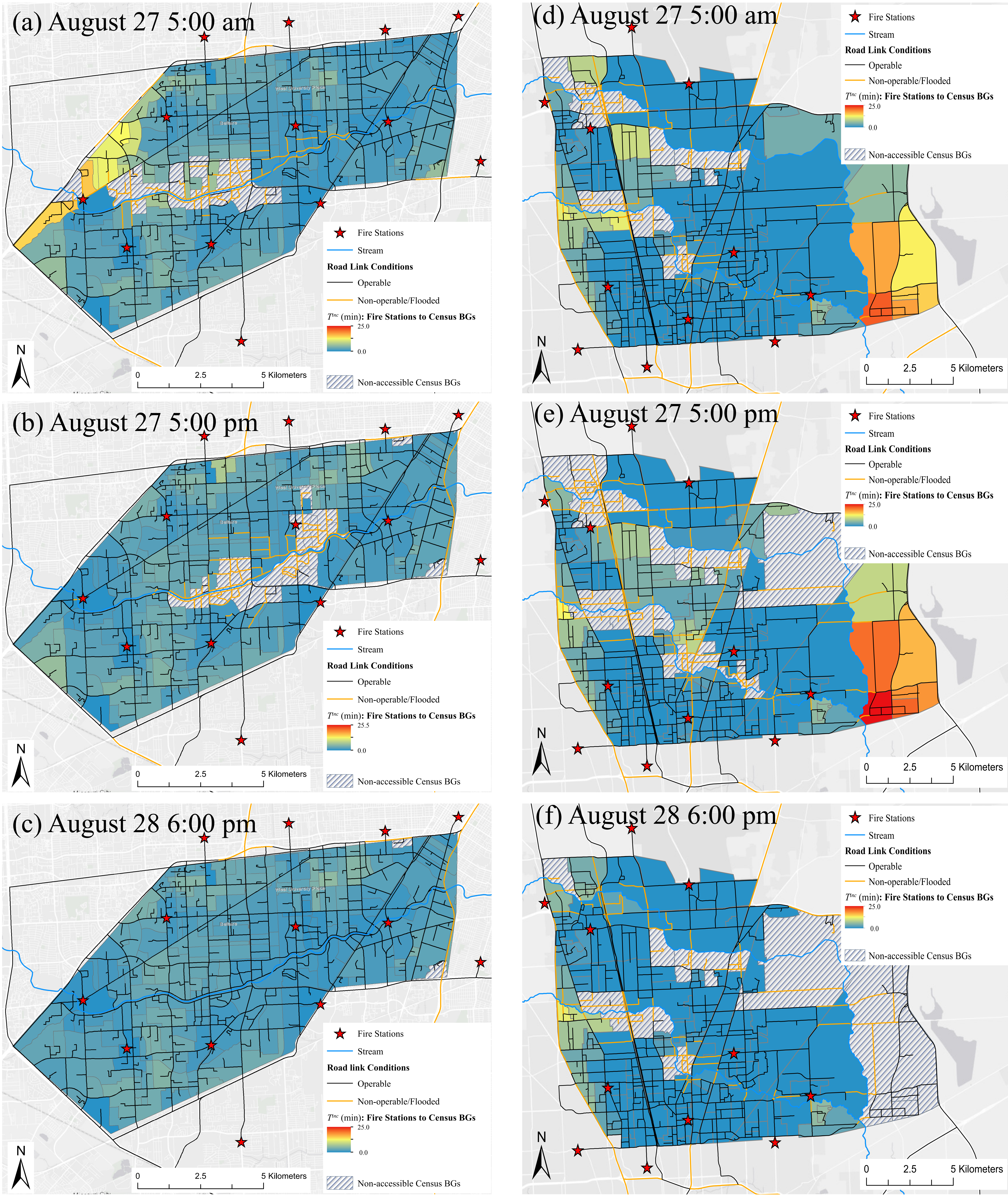
(a) August 27 5:00 am
(b) August 27 5:00 pm
(c) August 28 6:00 pm
(d) August 27 5:00 am
(e) August 27 5:00 pm
(f) August 28 6:00 pm
Fire Stations
Stream
Road Link Conditions
Operable
Non-operable/Flooded
T^{inc} (min): Fire Stations to Census BGs
25.0
25.5
0.0
Non-accessible Census BGs
N
0
2.5
5 Kilometers

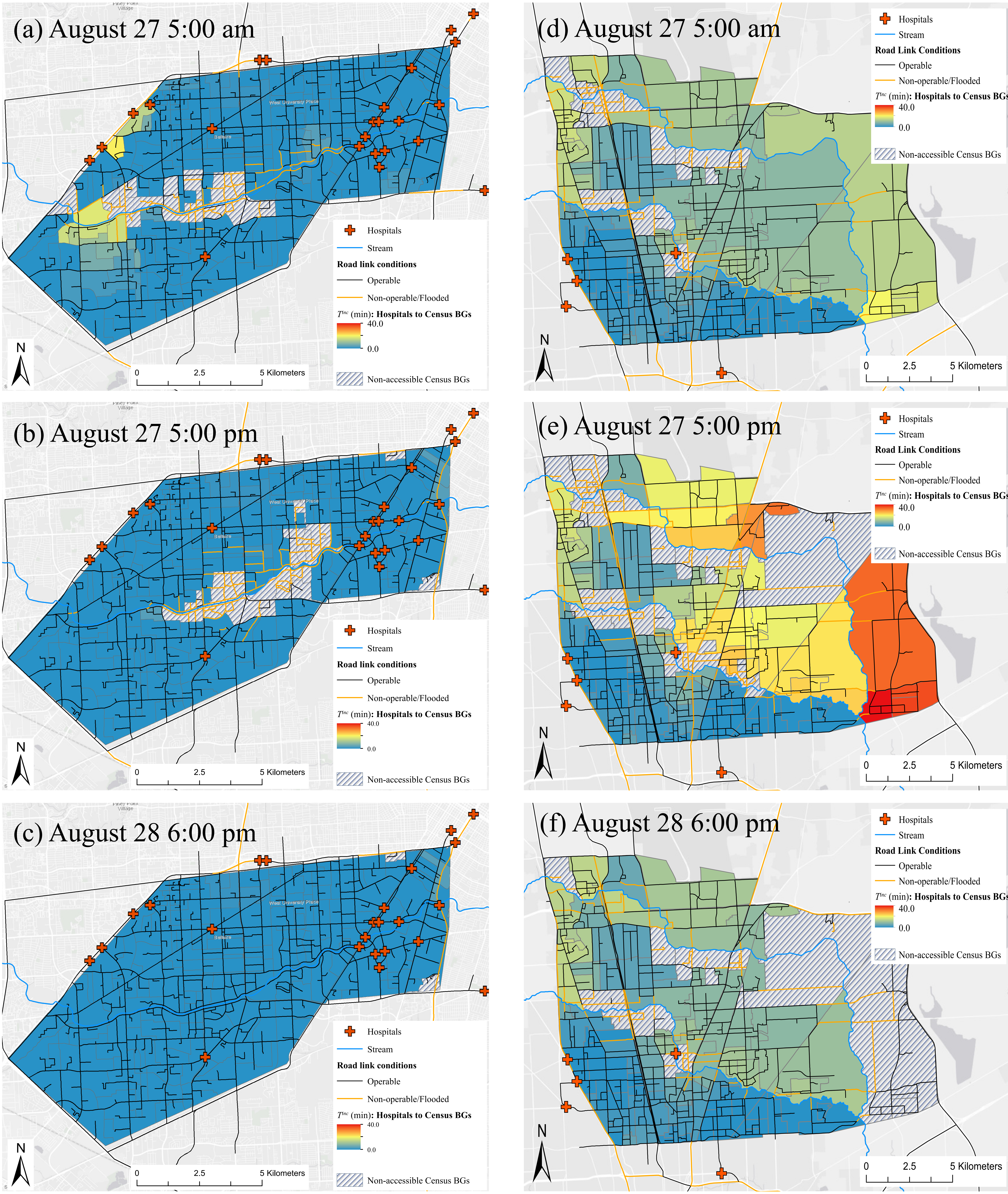
(a) August 27 5:00 am
West University Place
Bellaire
Hospitals
Stream
Road link conditions
Operable
Non-operable/Flooded
T^inc (min): Hospitals to Census BGs
40.0
0.0
Non-accessible Census BGs
N
0 2.5 5 Kilometers
(b) August 27 5:00 pm
Hospitals
Stream
Road link conditions
Operable
Non-operable/Flooded
T^inc (min): Hospitals to Census BGs
40.0
0.0
Non-accessible Census BGs
N
0 2.5 5 Kilometers
(c) August 28 6:00 pm
Hospitals
Stream
Road link conditions
Operable
Non-operable/Flooded
T^inc (min): Hospitals to Census BGs
40.0
0.0
Non-accessible Census BGs
N
0 2.5 5 Kilometers
(d) August 27 5:00 am
Hospitals
Stream
Road Link Conditions
Operable
Non-operable/Flooded
T^inc (min): Hospitals to Census BGs
40.0
0.0
Non-accessible Census BGs
N
0 2.5 5 Kilometers
(e) August 27 5:00 pm
Hospitals
Stream
Road Link Conditions
Operable
Non-operable/Flooded
T^inc (min): Hospitals to Census BGs
40.0
0.0
Non-accessible Census BGs
N
0 2.5 5 Kilometers
(f) August 28 6:00 pm
Hospitals
Stream
Road Link Conditions
Operable
Non-operable/Flooded
T^inc (min): Hospitals to Census BGs
40.0
0.0
Non-accessible Census BGs
N
0 2.5 5 Kilometers

Figure11

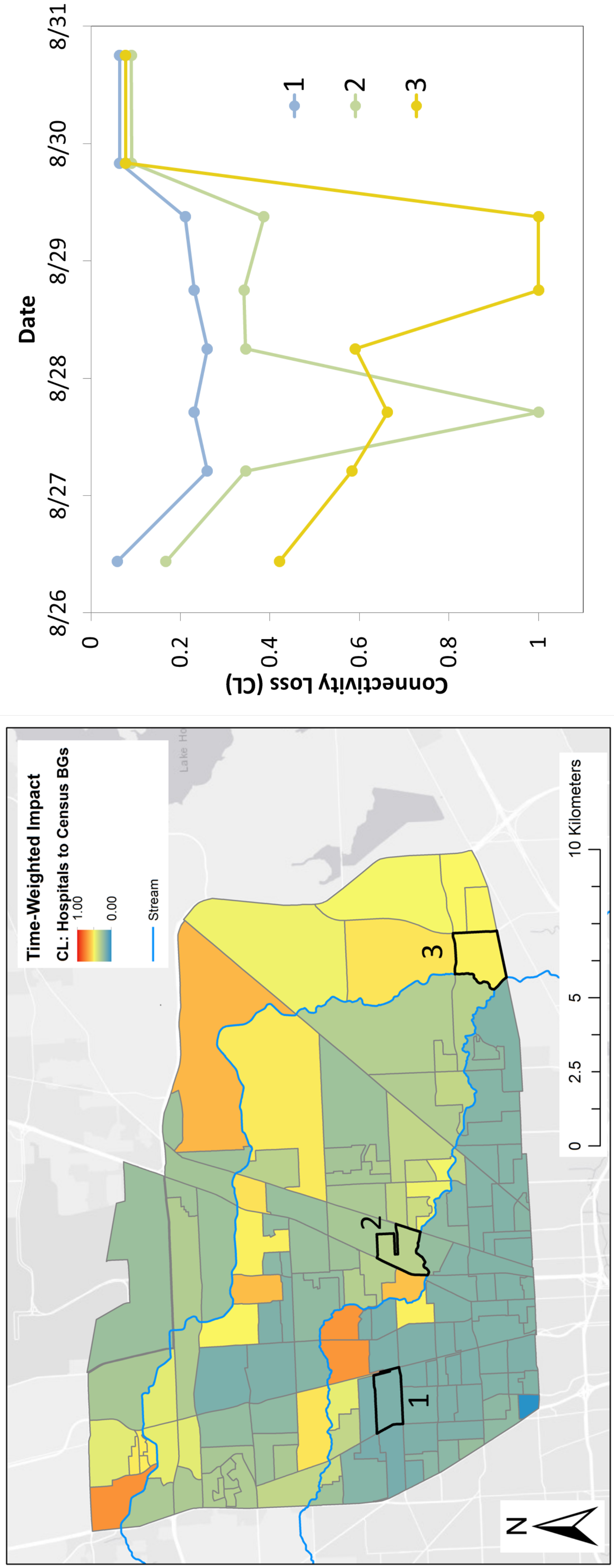

Date
8/26
8/27
8/28
8/29
8/30
8/31
Connectivity Loss (CL)
0
0.2
0.4
0.6
0.8
1
1
2
3
Time-Weighted Impact
CL: Hospitals to Census BGs
1.00
0.00
Stream
1
2
3
0
2.5
5
10 Kilometers
N

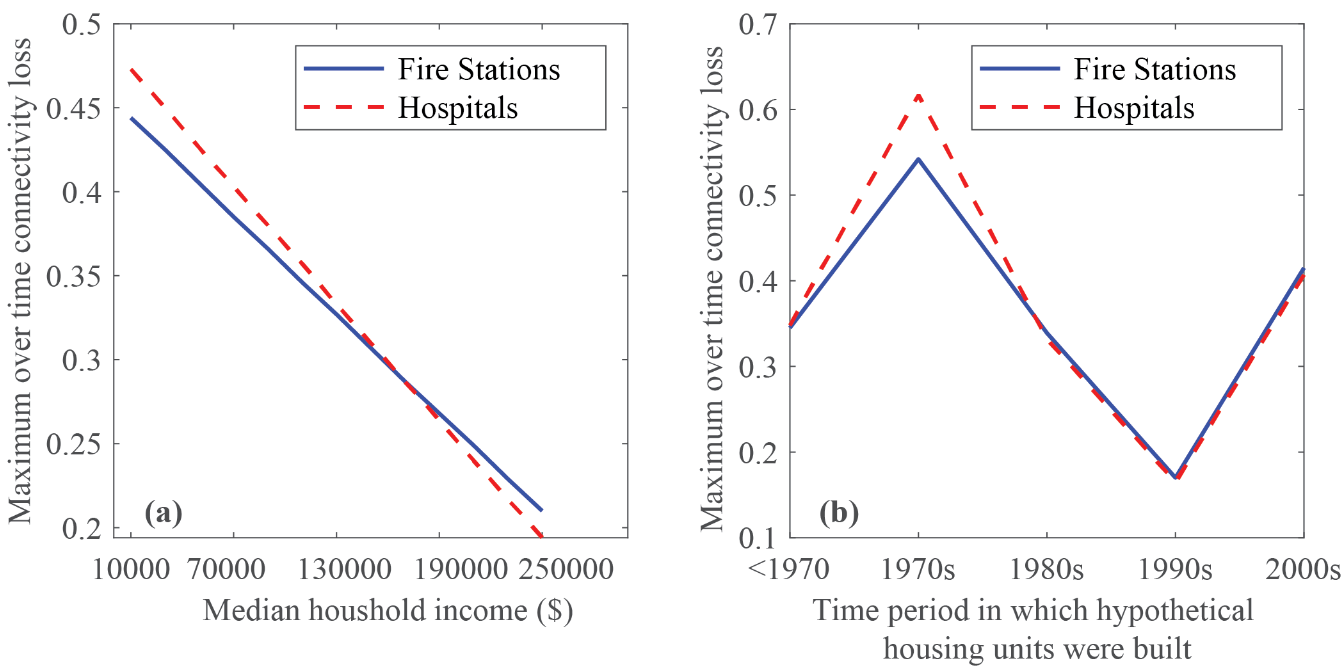
0.5
0.45
0.4
0.35
0.3
0.25
0.2
Maximum over time connectivity loss
Fire Stations
Hospitals
(a)
10000 70000 130000 190000 250000
Median houshold income ($)
0.7
0.6
0.5
0.4
0.3
0.2
0.1
Maximum over time connectivity loss
Fire Stations
Hospitals
(b)
<1970 1970s 1980s 1990s 2000s
Time period in which hypothetical
housing units were built

Figure13

Click here to access/download;Figure;Fig13.pdf

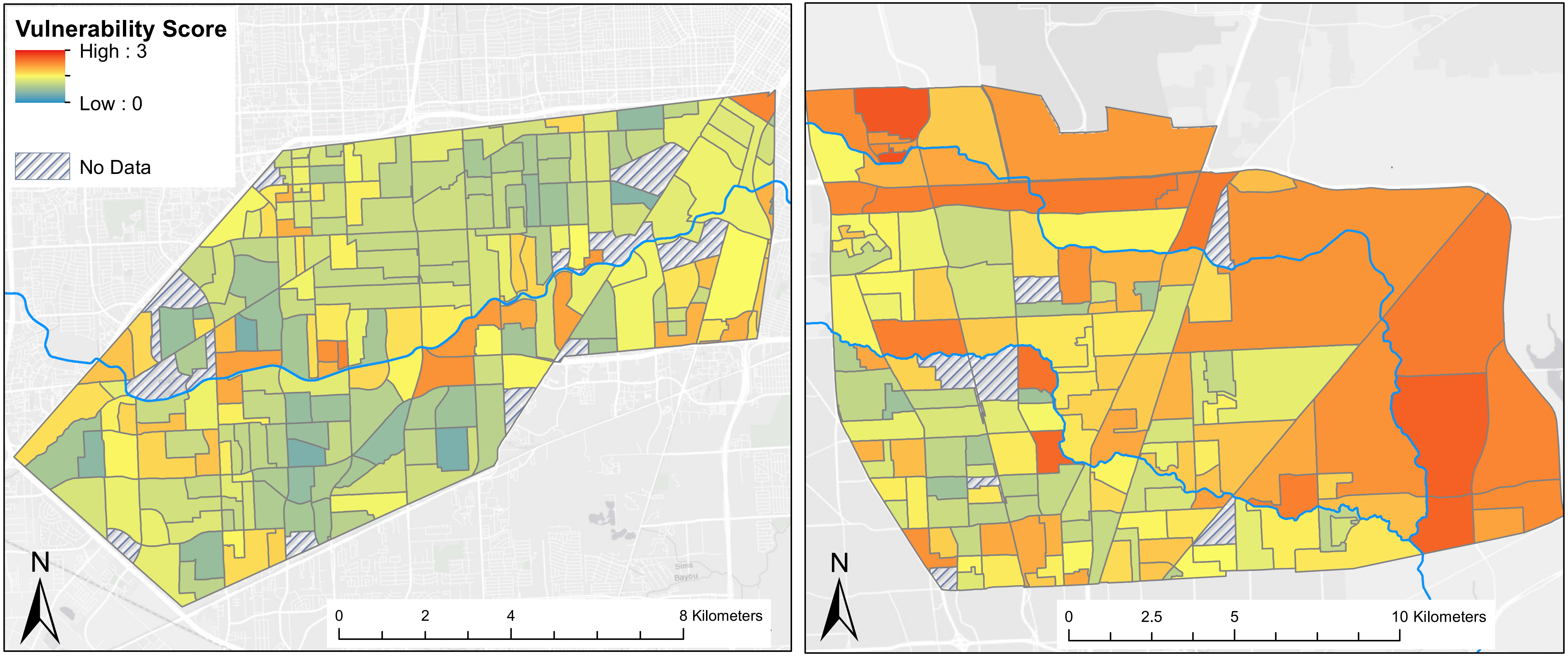

List of figures

Fig. 1. Locations of the case study areas

Fig. 2. Methodology flowchart

Fig. 3. (a) HEC-HMS model validation comparing modeled and observed peak streamflow in the Brays and Greens watersheds. (b) HEC-RAS model validation comparing modeled and observed peak depth in the Brays and Greens watersheds.

Fig. 4. Stage hydrograph comparisons between modeled and observed in (a) Brays and (b) Greens Bayou

Fig. 5. (a) Simple graph with its edge list and its representation by adjacency matrix **A** (Newman 2010) and (b) its flood-induced disrupted representation.

Fig. 6. Evolution of operational OD path ratios for (a) all routes r_1 and (b) routes within 1 mile of the bayou r_2 for the two case study areas.

Fig. 7. Maps of the average connectivity loss $\overline{CL}_{F\rightarrow BG}$ between fire stations and census block groups for Brays Bayou [parts (a), (b) and (c)] and Greens Bayou [parts (d), (e) and (f)] at three time instants during Hurricane Harvey: August 27 at 05:00 [parts (a) and (d)], August 27 at 17:00 [parts (b) and (e)], and August 28 at 18:00 [parts (c) and (f)].

Fig. 8. Maps of the average connectivity loss $\overline{CL}_{H\rightarrow BG}$ between hospitals and census block groups for Brays Bayou [parts (a), (b) and (c)] and Greens Bayou [parts (d), (e) and (f)] at three time instants during Hurricane Harvey: August 27 at 05:00 [parts (a) and (d)], August 27 at 17:00 [parts (b) and (e)], and August 28 at 18:00 [parts (c) and (f)].

Fig. 9. Maps of the travel time increase $T_{F\rightarrow BG}^{incr}$ between fire stations and census block groups at Brays Bayou [parts (a), (b) and (c)] and Greens Bayou [parts (d), (e) and (f)] at three time instants during Hurricane Harvey: August 27 at 05:00 [parts (a) and (d)], August 27 at 17:00 [parts (b) and (e)], and August 28 at 18:00 [parts (c) and (f)].

Fig. 10. Maps of the travel time increase $T_{H\rightarrow BG}^{incr}$ between hospitals and census block groups at Brays Bayou [parts (a), (b) and (c)] and Greens Bayou [parts (d), (e) and (f)] at three time instants during Hurricane Harvey: August 27 at 05:00 [parts (a) and (d)], August 27 at 17:00 [parts (b) and (e)], and August 28 at 18:00 [parts (c) and (f)].

Fig. 11. (a) Time-weighted connectivity loss ($CL_{H\rightarrow BG}^{tw}$) map between hospitals and census BGs for the duration of the storm, ranging from no loss at any point in the storm ($CL_{H\rightarrow BG}^{tw}=0$) to complete loss at every point during the storm ($CL_{H\rightarrow BG}^{tw}=1$). (b) Graph showing the time evolution of connectivity loss for select census blocks, ranging from low impact (#1) to high impact (#3).

Fig. 12. (a) Maximum over time connectivity loss by median household income of BGs in the Brays and Greens watersheds. (b) Maximum over time connectivity loss by time

period in which all hypothetical housing units were built in BGs in the Brays and Greens watersheds.

Fig. 13. Composite vulnerability scores by block group in the Brays (left) and Greens Bayou (right) study areas.